# SPSD II

# BIOGEOCHEMICHAL CYCLING OF CARBON, NITROGEN AND PHOSPHORUS IN THE NORTH SEA (CANOPY)

W. BAEYENS, L. CHOU, M. FRANKIGNOULLE, R. LAANE

PART 2

GLOBAL CHANGE, ECOSYSTEMS AND BIODIVERSITY

- ATMOSPHERE AND CLIMATE
- MARINE ECOSYSTEMS AND BIODIVERSITY
- TERRESTRIAL ECOSYSTEMS AND BIODIVERSITY
- NORTH SEA
- ANTARCTICA
- BIODIVERSITY

BIOGEOCHEMICHAL CYCLING OF CARBON, NITROGEN AND PHOSPHORUS IN THE NORTH SEA (CANOPY)

EV-20

SCIENTIFIC SUPPORT PLAN FOR A SUSTAINABLE DEVELOPMENT POLICY
(SPSD II)

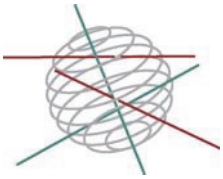

***Part 2:***
***Global change, Ecosystems and Biodiversity***

FINAL REPORT

# BIOGEOCHEMICAL CYCLING OF CARBON, NITROGEN AND PHOSPHORUS IN THE NORTH SEA CANOPY

**EV/20**


Natacha Brion, Marc Elskens, Sandra De Galan, Cristina Diaconu and Willy Baeyens
**ANCH - Vrije Universiteit Brussel**

Lei Chou, Claar van der Zee, Nathalie Roevros
**LOCGE – Université Libre de Bruxelles**

Alberto V. Borges, Laure-Sophie Schiettecatte, Bruno Delille and Michel Frankignoulle - deceased 13 March 2005
**Chemical Oceanography Unit, Université de Liège**

Remy W. P. M. Laane
**RIKZ (The Netherlands)**

Tom van Engeland –
**NIOO-CEME (The Netherlands)**


*January 2008*

BELGIAN SCIENCE POLICY


D/2007/1191/47
Published in 2007 by the Belgian Science Policy
Rue de la Science 8
Wetenschapsstraat 8
B-1000 Brussels
Belgium
Tel: +32 (0)2 238 34 11 – Fax: +32 (0)2 230 59 12
http://www.belspo.be

Contact person:
Mr David Cox
Secretariat: +32 (0)2 238 36 13

## TABLE OF CONTENTS

## ENGLISH SUMMARY

The CANOPY project aimed to determine the importance of the internal cycling processes of uptake and regeneration of carbon, nitrogen and phosphorus in the Southern Bight of the North Sea (SBNS), a marine area receiving riverine inputs from the Scheldt and Rhine rivers and influenced by inflowing English channel waters. The SBNS area was characterized by the presence of 2 large coastal river plumes with high levels of nutrients, and a central part with lower nutrient levels. Dissolved inorganic N (DIN and P (DIP) levels varied seasonally and were minimal for highest phytoplankton biomass, in spring and late summer. Additionally, organic N and P represented important fractions of the total N and P. In the central waters, dissolved organic N (DON), P (DOP) and particulate organic P (POP) dominated the N and P pools in summer, but their relative importance was more limited in the river plumes. For the pelagic system, DIC, DIN and DIP varied seasonally and were highest during the spring phytoplankton bloom, and for some stations, at the end of the summer phytoplankton bloom. Additionally, the uptake of DIN and primary production (PP) were well correlated with a C:N ratio of 6.5 very close to the Redfield ratio. In general, the regeneration of DIN largely exceeded the uptake except in spring, where a more balanced situation was observed. The regeneration of DIP also represented a large fraction of the DIP uptake. Heterotrophic processes are thus very active in the SBNS. They clearly dominate the pelagic N cycling, and are in balance with uptake processes for DIP. At ecosystem scale, it was demonstrated that the Scheldt plume was net heterotrophic during most years and acted as an important source of $CO_2$ for the atmosphere. In contrast, the Scheldt plume also acted as an active sink for both DIN and DIP probably due to active denitrification and physical adsorption processes in this organic matter and SPM rich environment. In contrast, the central waters were on the yearly average autotrophic and acted as a sink for $CO_2$. Again in contrast, there was a net production of DIN and DIP. The comparison of DIN and DIP budgets with DIC budgets showed that correlations exist but were not straightforward. In general, correlations showed a C:N ratio of 3.5 (<Redfield) and a C:P ratio of 109 (=Redfield). This suggests that whatever the season there is a DIC production sustained by OM with a high C:N ratio, either of terrestrial (estuarine) origin or from the sediment. This is agreement with the fact that consumption of DIC by PP exceeds the net ecosystem DIC production. The other possible cause is a large removal of DIN by denitrification in agreement with the fact that net pelagic DIN production largely exceeds net ecosystem DIN production. However, the correlation lines did not pass through 0 showing that primary production and respiration are not the only players in the DIC-DIN-DIP dynamics with the presence of unrelated DIC, DIN and DIP sources our sinks.

## DUTCH SUMMARY

Het CANOPY project had als doel het belang aan te tonen van de interne cyclische processen van opname en regeneratie van C, N en P in de Zuidelijke Bocht van de Noordzee (SBNS). Dit zeegebied krijgt een enorme toevoer van rivierwater van de Schelde en de Rijn te verwerken en wordt beinvloed door water dat binnenkomt via het Engelse Kanaal. Het SBNS gebied werd gekenmerkt door de aanwezigheid van 2 grote rivierpluimen met hoge concentraties aan nutrienten en een centraal gedeelte met lagere hoeveelheden aan nutrienten. Opgeloste anorganische N (DIN) en P (DIP) hoeveelheden varieerden seizonaal en waren het laagst wanneer de phytoplankton biomassa het hoogst is, dwz. in de lente en de late zomer. Organische N en P vertegenwoordigden belangrijke fracties van de totale hoeveelheid N en P aanwezig. In het centrale gedeelte van het SBNS overheersten de hoeveelheden aan opgeloste organische N (DON) en P (DOP), en particulair organische P (POP) de N en P pools in de zomer, maar hun relatief belang was beperkter in de rivierpluimen. In het pelagische systeem varieerden DIC, DIN en DIP opnamen seasonaal en waren het hoogst tijdens de fytoplanktonbloei in de lente. Voor een aantal stations waren deze ook het hoogst tijdens de fytoplanktonbloei op het einde van de zomer. De opname van DIN en de primaire productie (PP) zijn zeer goed met elkaar gecorreleerd met een C:N verhouding van 6.5 (=Redfield). Over het algemeen overheerste de regeneratie van DIN zeer sterk de opname van DIN behalve in de lente, wanneer een goed evenwicht tussen beide werd waargenomen. De regeneratie van DIP vertegenwoordigde een belangrijke fractie van de opname van DIP. Men kan dus zeggen dat heterotrofe processen zeer actief zijn in de SBNS. Deze overheersten zeer duidelijk de pelagische N cyclus en waren in evenwicht met de opnameprocessen van DIP. Er werd aangetoond dat de Scheldepluim net heterotroof was gedurende het grootste gedeelte van het jaar en dat het een belangrijke bron van $CO_2$ was voor de atmosfeer. In tegenstelling, de Scheldepluim trad ook op als een actieve poel (sink) voor DIN en DIP hoogst waarschijnlijk door de actieve denitrificatie en fysische adsorptie processen die plaatsgrijpen in dit milieu rijk aan organisch materiaal en SPM. In tegenstelling, het centrale gedeelte was op jaarbasis autotroof en trad op als een poel voor $CO_2$. Anderzijds werd vastgesteld dat er hier een netto productie van DIN en DIP was. Een vergelijking van de DIN en DIP budgetten met deze van DIC toonden aan dat er een correlatie bestaat tussen beide. Over het algemeen toonden deze correlaties een C:N verhouding van 3.5 (<Redfield) en een C:P verhouding van 109 (=Redfield) aan. Dit veronderstelt dat er, onafgezien van het seizoen, een DIC productie is met een hoge C:N verhouding die in stand wordt gehouden door OM dat ofwel een terrestrische (estuarium) oorsprong heeft ofwel afkomstig is van de sedimenten. Dit is in overeenstemming met het feit dat het verbruik van DIC hoger is dan de netto DIC productie van het systeem. Een andere

mogelijke oorzaak is een zeer groot verbruik van DIN door denitrificatie wat in overeenstemming is met de netto pelagische DIN productie die de netto ecosysteem DIN productie in hoge mate overschrijdt. De correlatielijnen gaan echter niet door de oorsprong wat aantoont dat naast primaire productie en respiratie er nog andere processen een rol spelen in de DIC-DIN-DIP dynamiek. Bovendien zijn de bronnen en poelen van DIC, DIN, en DIP niet gekoppeld aan elkaar.

# 1. INTRODUCTION

The inputs of organic material and nutrients via rivers provide a significant contribution to the global marine carbon, nitrogen, phosphorus and silicon budgets (e.g., Sempéré et al., 2000; Beusen et al., 2005; Harrison et al., 2005). However, before this material reaches the open ocean, intense biogeochemical transformations take place in estuaries, delta's and the open shelf (Siefert, 2004). As a result the quantity, origin and quality of the organic matter and nutrients that actually reach the open ocean may differ substantially from that delivered to upper estuaries. Biogeochemical processing may remove a significant fraction of the river nutrient load by e.g. nitrification-denitrification, or by uptake by phytoplankton and bacteria. Over the last century nitrogen and phosphorus discharges to the aquatic environment have increased dramatically due to human activities and population growth (Herbert 1999, Hulth et al. 2005) but it is believed that the situation should improve in Europe. The river N flux for example is likely to decrease by ~20 % over the coming 3 decades (Bouwman et al., 2005) in Europe. The important biogeochemical processes involved are, however, insufficiently quantified; causing global extrapolations to have a large uncertainty (e.g., for the $CO_2$ budget see Borges, 2005 and Borges et al., 2005; 2006). Many elementary data regarding the origin, fluxes and biogeochemical transformations of C, N, P and Si in coastal systems are simply lacking and extrapolations based on available data are not valid. Estimates of actual delivery to the coastal zone and of the high impact of human perturbations (Downing et al., 1999) remain speculative unless detailed insight in estuarine and open shelf biogeochemical processes is acquired. It is to this global perspective that the CANOPY research project is contributing.

Coastal ecosystems in industrialized densely populated areas, like the Southern Bight of the North Sea (SBNS), are subjected to increased organic matter (OM), dissolved inorganic carbon (DIC) and nutrient inputs via rivers, sewage and atmospheric deposition which may entail mass production of algae (i.e. eutrophication) which in turn, when decomposing, can result in oxygen depletion (hypoxia) or even anoxia, for the extreme cases. Sources, input trends and internal cycling processes of nutrients have been studied for many years in this system in the framework of large national (Belgian) and international projects. A large amount of information has been obtained but severe gaps and uncertainties are still prevailing, hampering our global understanding of the biogeochemistry of the system.

The Southern Bight of the North Sea (fig. 1) is a marine area receiving carbon and nutrients from river inputs (Rhine and Scheldt mainly), atmospheric deposition, and exchanges with the Atlantic Ocean through the English channel. Sources of nutrients and carbon are mostly linked to anthropogenic activities (agriculture, industries, domestic wastewater). The most recent Quality Status Report (OSPARCOM, 2000)

for the Greater North Sea highlighted very high inputs of nitrogen and phosphorus to the North Sea. These nutrients and carbon are subject to internal fluxes and processes like internal recycling of organic and inorganic compounds, uptake by phytoplankton, mineralization, atmospheric efflux, sedimentation, but recent average data for the North Sea dealing with these internal N, P and C recycling processes are rather scarce. In this project we study the relative importance of major processes involved in these cycles in order to be able to understand the global functioning of the concerned ecosystem.

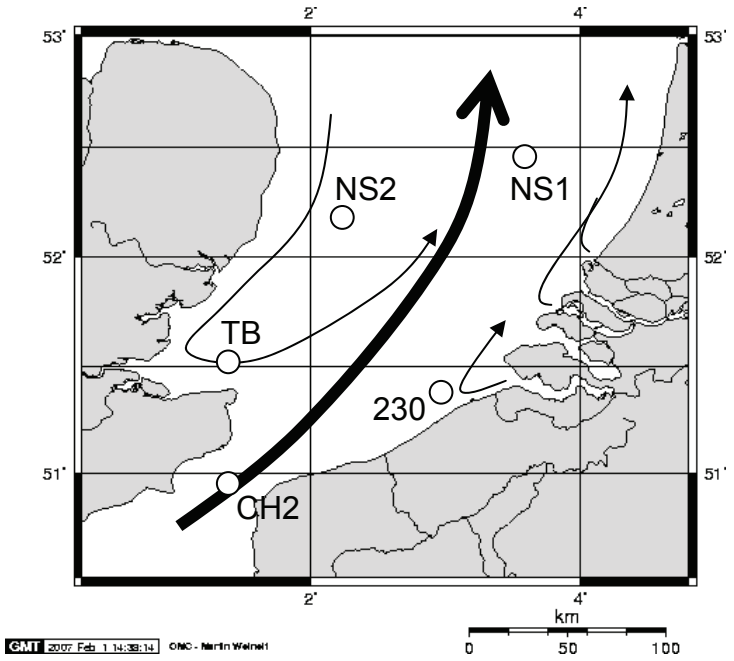


Fig.1. Southern Bight of the North Sea with main water circulation (arrows) and position of the process stations.

The Southern Bight of the North Sea (fig. 1) corresponds to the southern part of the open North Sea located between the Strait of Dover and 52.5°N latitude line, as defined in OSPARCOM 2000. This 20,000 km² area is relatively shallow (20 to 30m) with a well mixed water column throughout the year. It is surrounded by the coastlines of South-Eastern England, The Netherlands, Belgium, and Northern France. Seawater flows from the English channel to the North through the central part of the area, western coastal waters flow southwards along the English coast until the Thames Bay before joining the main northward seawater flow, while eastern coastal waters flow northwards along the Dutch coast (OSPARCOM 2000). These eastern coastal waters receive the waters of two large rivers: the Scheldt (average discharge 100 $m^3s^{-1}$) and the Rhine-Maas (average discharge 1400 $m^3s^{-1}$), both draining densely populated and industrialized areas.

## 2. AIM OF THE PROJECT

The general objective of this project is to determine the importance of the internal cycling processes of uptake and regeneration of carbon and nutrients (N and P) in the Southern Bight of the North Sea. These will be compared to the inputs and outputs of C-N-P in order to visualize the global functioning of the considered ecosystem. Moreover, the relative importance of the most important C-N-P compounds (organic/inorganic and dissolved/particulate) in these processes will be investigated.

More specifically, we will focus:

- On the in situ assessment of DIN, DIP and DIC uptake and regeneration rates using different tracer techniques (stable and radio-active isotopes.
- On whole ecosystem budgets for dissolved inorganic carbon, that should allow an estimation of Net Ecosystem Production (NEP) and provide air-sea $CO_2$ exchange budgets based on high temporal and spatial data sets.
- On whole ecosystem budgets for dissolved inorganic nitrogen and phosphorus, that should allow an estimation of the net filtering effect of the SBNS.

# 3. METHODS

## 3.1. CRUISES AND SAMPLING

Seven five-days cruises were carried out onboard the RV BELGICA between September 2003 and October 2004:
BG03-21: 1-5/09/2003 (end of summer)
BG03-27: 27 to 31/10/2003 (autumn)
BG03-32: 8-12/12/2003 (winter)
BG04-03: 23 -27/02/2004 (late winter)
BG04-07: 29/03-02/04/2004 (early spring)
BG04-12: 24-28/05/2004 (spring)
BG04-22: 04-08/10/2004 (autumn)
Water samples were taken at 5 fixed stations (Tab. 1 and Fig. 1) at a depth of 2 m using a 30L Go-Flo bottle for concentrations (see 3.2) and process measurements (see 3.3). At the same stations vertical profiles of temperature, salinity and light intensity were recorded with a Seacat SCTD SBE19 system.
Additionally, surface waters samples were collected along the ship track with a frequency of 1 minute (for $pCO_2$ and $O_2$ determinations) to half-an-hour (for dissolved inorganic nitrogen and phosphate, and total alkalinity determinations) from the surface seawater supply of the ship (pump inlet at a depth of 2.5 m). Salinity and temperature corresponding to these samples were measured using a SeaBird® SBE21 thermosalinograph. For each of the cruises, the track was chosen in order to obtain the best surface coverage.

Table 1. Coordinates of the fixed stations

| Station | Longitude (°W) | Latirude (°N) |
|---|---|---|
| St230 | 2°50 | 51°20 |
| NS1 | 3°30 | 52°29 |
| NS2 | 2°20 | 52°09 |
| TB | 1°27.5 | 51°31 |
| CH2 | 1°15 | 50°55 |

## 3.2. CONCENTRATION MEASUREMENTS

### 3.2.1. Phosphorus speciation

Dissolved phosphorus species were determined after filtration through pre-combusted (500ºC, 4 h) GF/F filters, which were used for the particulate phosphorus speciation. Soluble reactive phosphorus, hereafter phosphate ($PO_4$), was measured

according to the method of Grasshoff et al. (1983). Dissolved inorganic phosphorus (DIP) was determined as $PO_4$ after digestion with 9N $H_2SO_4$ (120ºC, 30 min). DIP comprises $PO_4$ and polyphosphates (poly-$PO_4$), although hydrolysis of acid-labile organic phosphorus compounds may also contribute to this parameter. Poly-$PO_4$ was determined as the difference between DIP and $PO_4$. Total dissolved phosphorus (TDP) was measured by wet oxidation in acid persulphate (120ºC, 30 min) (Grasshoff et al., 1983). Dissolved organic phosphorus (DOP) was subsequently calculated as the difference between TDP and DIP. Filters for total particulate phosphorus (TPP) determination were combusted at 500$^{o}$C for 1.5 h with $MgSO_4$ and subsequently extracted in 1 N HCl for 24 h (Solorzano and Sharp, 1980). Filters for particulate inorganic phosphorus (PIP) were extracted in 1 N HCl for 24 h. Particulate organic phosphorus (POP) was calculated as the difference between TPP and PIP. Additionally, the unfiltered water sample was digested by wet oxidation in acid persulphate, which gives the total phosphorus (TP).

### 3.2.2. Nitrogen speciation

Ammonium, nitrate, and nitrite were determined after filtration through pre-combusted (500ºC, 4 h) GF/F filters with colorimetric methods. Ammonium is measured with the indophenol blue technique according to Koroleff (1969). Nitrate and nitrite are determined in acid preserved samples with a Technicon auto analyzer II system according to Elskens and Elskens (1989). Particulate matter is collected by filtration on pre-combusted (500ºC, 4 h) GF/F filters. The filters were dried for 8h at 50°C and particulate organic nitrogen (PN) was determined with a Carlo Erba C/N analyzer (Pella, 1991). The dissolved organic nitrogen (DON) assessment relies on the combination of a total dissolved nitrogen (TDN) and an independent dissolved inorganic nitrogen (DIN = nitrate + nitrite + ammonium) determination. TDN is determined as nitrate after peroxodisulphate oxidation of the dissolved nitrogen compounds (originally described by Valderama, 1981) in a microwave oven (Dafner et al., 1999).

### 3.2.3. Chlorophyll *a*

Chl a was measured on GF/F filters after filtration of 250-ml seawater under low suction, following the fluorometric method of Yentsch & Menzel (1963). For analysis, the filters were extracted with 90% acetone at -20°C for 24 h. Samples were centrifuged (10 min, 5500 rpm) and the fluorescence of the extract was measured with a Shimadzu RF-150 fluorometer, using an excitation wavelength of 430 nm and an emission wavelength of 663 nm. The fluorescence was calibrated with a stock solution of pure chlorophyll a (Merck).

### 3.2.4. Dissolved inorganic carbon and oxygen

Underway parameters (salinity, temperature and partial pressure of $CO_2$ ($pCO_2$)) were sampled with a 1 minute frequency from the surface seawater supply of the ship (pump inlet at a depth of 2.5 m). Salinity and temperature were measured using a SeaBird® SBE21 thermosalinograph. $pCO_2$ was measured by means of a non-dispersive infrared gas analyzer (IRGA, Li-Cor®, Li-6262) and an equilibrator (Frankignoulle et al. 2001). The IRGA was calibrated daily using pure nitrogen (Air Liquide Belgium) and two gas mixtures of a $CO_2$ molar fraction of 366 and 810 ppm (Air Liquide Belgium), calibrated against two National Oceanic and Atmospheric Administration (NOAA) standards with a $CO_2$ molar fraction of 361 and 774 ppm. The temperature at the outlet of the equilibrator was monitored with a platinum resistance thermometer (PT100, METROHM®), with an estimated accuracy of ±0.05°C. The $pCO_2$ values were corrected for the temperature difference between *in-situ* seawater and water in the equilibrator using the algorithm proposed by Copin-Montégut (1988; 1989) and then corrected to the local barometric pressure. The accuracy of the $pCO_2$ measurement by equilibration was estimated to ±2 µatm (cumulated errors on temperature correction and instrument calibration). Oxygen ($O_2$) concentrations were measured with a 1 min frequency using a galvanic electrode calibrated daily against discrete samples measured using the Winkler method. The oxygen saturation level ($\%O_2$) was computed from the observed concentration of dissolved $O_2$ and the concentration of $O_2$ at saturation calculated according to Benson and Krause (1984). The accuracy of $O_2$ measurements was ± 0.5 µmol $kg^{-1}$ (0.2% of level of saturation). Total alkalinity (TA) discrete surface samples were measured with the Gran electrotitration method. The accuracy of TA measurements was ± 3 µmol $kg^{-1}$. Dissolved inorganic carbon (DIC) was computed from $pCO_2$ and TA measurements using carbonic acid constants given by Roy et al. (1993), dissociation constants of boric acid given by Dickson (1990) and the $CO_2$ solubility coefficient ($\alpha$) given by Weiss (1974). The accuracy on DIC computed from TA and $pCO_2$ was ± 5 µmol $kg^{-1}$ (estimated from cumulated errors on TA and $pCO_2$).

The air-sea $CO_2$ flux ($F_{CO2}$) was computed from the $pCO_2$ air-sea gradient ($\Delta pCO_2$ = $pCO_2$ - $pCO_{2atm}$, where $pCO_{2atm}$ refers to values in the atmosphere), $\alpha$, and the gas transfer velocity ($k$) according to:

$$F_{CO2} = \alpha\, k\, \Delta pCO_2 \qquad (1)$$

We used nominally the $k$ parameterization as function of wind speed ($u_{10}$) given by Nightingale et al. (2000), established in the North Sea. For comparative purposes with previous studies, computations were also carried out with the $k$ parameterizations as function of wind speed given by Liss and Merlivat (1986), Wanninkhof (1992), and Wanninkhof and McGillis (1999).

## 3.3. PROCESS MEASUREMENTS

### 3.3.1. Primary Production

Dissolved inorganic carbon (DIC) uptake was essayed by incubation of $^{14}$C-bicarbonate spiked seawater. During kinetic experiments, seawater was incubated under constant light conditions (~150 µmol quanta $m^{-2}$ $s^{-1}$) for 2, 4, 8, 12 and 24 hrs. Additional incubations were done using inhibitors. Photosystem II was blocked with 3-(3,4-dichlorophenyl)-1,1-dimethylurea (DCMU) using a final concentration of 24 µM, thus preventing photosynthetic DI$^{14}$C uptake. The metabolic inhibitor sodium azide was used to stop all biological activity (46 µM, final concentration). Incubations were stopped by filtration on Whatman GF/F-filters. Filters were acidified with HCl, dried and stored until counting in the home laboratory. Radioactivity on the filters and in the standards was counted in a liquid scintillation counter using ReadySafe as scintillation cocktail.

Production versus irradiation curves were obtained by incubation of 14 aliquots with under a light gradient and in the dark for 2-4 hours. The Chl *a* normalized DIC uptake rate versus light intensity can be described with the Platt equation (Platt *et al*., 1980):

$$P^B = P^B_{\max} (1 - e^{-\alpha E / P^B_{\max}}) e^{-\beta E / P^B_{\max}} \quad (2)$$

where $P^B$ is the photosynthetic rate in µg C (µg Chl *a*)$^{-1}$ $h^{-1}$, $P^B_{max}$ is the maximum photosynthetic rate in the same units as $P^B$, $\alpha$ the maximum light utilization coefficient in µg C (µg Chl *a*)$^{-1}$ $h^{-1}$ (µmol quanta $m^{-2}$ $s^{-1}$)$^{-1}$, $\beta$ the photoinhibition parameter in the same units as $\alpha$, and E the photosynthetically available radiation (PAR) in µmol quanta $m^{-2}$ $s^{-1}$.

The depth integrated primary production was calculated using the photosynthetic parameters obtained from the P-E curve fit, the Chl *a* concentration and the light availability at each depth. The incident light and day length were derived theoretically from the geographical position of the station and the date of sampling. The attenuation coefficient was deduced from the *in situ* measured light profile. The photoinhibition term of the Platt equation was not included in the fit of the P-E curves as this process was not of any importance during the incubations.

### 3.3.2. Phosphate uptake

Seawater samples were spiked in triplicate with $^{33}PO_4$. $PO_4$ uptake was measured in a kinetic experiment under constant light conditions in September and October 2003 and in March and October 2004. Uptake of $PO_4$ was determined in different size fractions: 0.2-2 µm, 2-12 µm and >12 µm. Incubations with antibiotics, azide and DCMU were performed like in the carbon uptake experiments. The fraction of P

uptake due to abiotic processes such as passive adsorption is estimated by incubation amended with azide. Biological $PO_4$ uptake is the total $PO_4$ uptake minus the $PO_4$ uptake after addition of azide. Incubations with the addition of DCMU give an estimate of the importance of photosynthetic versus non-photosynthetic rates of assimilation. Additionally, the $^{33}PO_4$ assimilation in the dark was determined. The contribution of heterotrophic bacteria to the P uptake was investigated by experiments using antibiotics. A mixture of the antibiotics streptomycine and polymyxine B (0.01% final concentration) was added to inhibit bacterial activity. Streptomycine is an inhibitor of prokaryotic protein synthesis, whereas polymyxine B kills gram-negative bacteria through the disruption of their cell-membrane. Incubations were stopped by filtration on nuclepore membrane filters, which were rinsed with filtered seawater containing 5 µM $PO_4$ and filtered seawater. The standards and the dried filters were counted in a liquid scintillation counter using ReadySafe as a scintillation cocktail.

### 3.3.3. Regeneration of $PO_4$ by 3 5' Nucleotidase activity

Regeneration of $PO_4$ was assessed using the 5'-nucleotidase (5PN) method of Ammerman (1993). Enzymatic liberation of $^{32}PO_4$ from [γ-$^{32}$P]ATP and its subsequent uptake was assayed in triplicate at *in situ* temperature in the light. Four fractions were incubated with [γ-$^{32}$P]ATP for 2-4 hours: seawater pre-filtered on 0.2 µm and 2 µm nuclepore filters, unfiltered seawater and formaline-killed seawater. The spiked samples were filtered on 0.2 µm nuclepore filters, the filters were rinsed with filtered seawater and the $^{32}$P on the filters was counted (total particulate $^{32}$P). The filtrate was subsampled for $^{32}$P counting (total dissolved $^{32}$P) and activated charcoal and sulphuric acid were added to the remainder of the filtrate. This slurry was filtered on Millipore HA filters (0.45 µm) and $^{32}$P was counted in the filtrate ($^{32}PO_4$). Subsequently, the 5PN activity can be calculated and the percent of $^{32}PO_4$ taken up after liberation due to the hydrolysis of $^{32}$P-ATP by 5PN.
The 5PN activity in the dissolved fraction was subtracted from the activity in the <2 µm and the activity in the <2 µm fraction was subtracted from the total activity to obtain the 5PN activities in the small particulate fraction (0.2-2 µm) and the large particulate fraction (>2 µm), respectively. The same was done for the $^{32}PO_4$ uptake in the two particulate fractions. Dried filters, filtrate aliquots and standards were counted in a liquid scintillation counter using ReadySafe as a scintillation cocktail.

### 3.3.4. Alkaline phosphatase activity

The alkaline phosphatase (AP) activity assay was performed using 4-methylumbelliferyl-phosphate (MUF-$PO_4$) as the fluorogenic substrate according to

Hoppe (1983). Seawater samples were incubated with MUF-$PO_4$ in the dark at *in situ* temperature. Time zero control samples were taken for all concentrations added at each station and season, as the extent of the spontaneous non-enzymatic hydrolysis of the MUF-P substrate increases with the amount substrate concentration added and the ratio between the two varies from site to site (Sebastian and Niell, 2004). The evolution of the fluorescent product MUF was followed in kinetic assays performed in triplicate after 0, 1, 2 and 4 hours. AP activity was calculated by linear regression from the first three kinetic points. When not immediately measured on board, the samples were preserved with $HgCl_2$ (4mM final concentration) and stored frozen until analysis in the laboratory (Christian and Karl, 1995). Furthermore, seawater samples, pre-filtered on 0.2 µm, 2 µm and 12 µm nuclepore filters, were incubated with MUF-$PO_4$ at stations 230 and NS1. During the May and October 2004 cruises, kinetic parameters were determined ($V_{max}$ and $K_m$+$S_n$) and fluorescence was measured directly onboard using a Shimadzu fluorometer.
The turnover time $T_a$ of substrate in the incubation bottle was computed using equation 3 following Thingstad et al. (1993):

$$T_a = \frac{t}{-\ln(1-R)} \tag{3}$$

where $T_a$ = ($S_a$+$S_n$)/V is the turnover time in the sample with added and natural substrate concentration $S_a$ and $S_n$ respectively; V is the velocity of the reaction; t is the incubation time; R is the consumed fraction of the added MUF-$PO_4$. Then, following Wright and Hobbie (1966), the Michaelis-Menten equation can be rearranged to:

$$T_a = \frac{K_m + S_n}{V_{\max}} + \frac{S_a}{V_{\max}} \tag{4}$$

where $V_{max}$ is the maximum enzyme activity (in nM $h^{-1}$), and $K_m$ is the value of S for which V is half of $V_{max}$. $K_m$ and $V_{max}$ were estimated from a modified Lineweaver-Burk plot.

### 3.3.5. Ammonium uptake, nitrate uptake and ammonium regeneration

Isotope dilution and enrichment incubation experiments were performed using $^{15}N$ labeled dissolved inorganic nitrogen (DIN = $NH_4^+$ or $NO_3^-$). Incubations were done for 250 ml samples in transparent plastic polycarbonate bottles submerged in an incubator with continuously flowing water to ensure ambient temperature and with constant artificial light intensities (~150 µmol quanta $m^{-2}$ $s^{-1}$). Samples are spiked with $^{15}N$-$NH_4^+$ or $^{15}N$-$NO_3^-$ (around 10 % final $^{15}N$ abundance), incubated for 6 hours, and filtered on combusted GF/F glass-fiber filters (Whatman). The filters are dried at 50°C for 8 hours prior to analysis of PON and $^{15}N$-PON abundance. The filtrates are used to determine final $NH_4^+$ and $NO_3^-$ concentration and for the samples incubated with

$^{15}NH_4^+$ for 6 hours, additionally the filtrate is kept frozen until analysis of final $^{15}N$-$NH_4^+$ abundance (Diaconu et al. 2005). In all cases, $^{15}N$ abundances and PON concentrations are measured using an elemental analyzer (Carlo-Erba C/N analyzer) coupled via a conflo-interface to an isotope ratio mass spectrometer (Finnigan Delta-Plus XL) (Nieuwenhuize et al. 1994).

Initial and final $^{15}N$-abundance and concentration data for the $NH_4^+$, $NO_3^-$ and PON pools obtained from the 3 incubation experiments were used simultaneously in an isotopic mass-balance model in order to compute $NH_4^+$ and $NO_3^-$ uptake rates, and ammonification rates. The model is a 3 compartment open model allowing the assessment of exchange rates between the considered compartments: $NH_4^+$, $NO_3^-$ and PON. This model assumes that exchange between compartments is governed by first order differential equations with constant coefficients of the general type:

$$\frac{d\,{}^{p}X_i}{dt} = \sum_{j\neq i}^{n} k_{ji} \cdot {}^{p}X_j - \sum_{j\neq i}^{n} k_{ij} \cdot {}^{p}X_i \qquad (5)$$

where $X_i$ is the nitrogen concentration of isotope p ($^{14}N$ or $^{15}N$) within compartment i at time t, $k_{ij}$ is the rate constant for exchange from compartment i to compartment j (in reciprocal time units), p is the isotope $^{15}N$ or $^{14}N$ and n represents the number of compartments (3 in this case: $NH_4^+$, $NO_3^-$ and PON).

The equation above states that the net content in any compartment i equals the sum of all inflows from the other compartments minus the sum of all outflows towards the other compartments. These mass balance differential equations have been solved numerically as described in Elskens et al. (1988). Values for the rate constants are obtained using weighted least squares techniques as described in Elskens et al. (2005). Rates for initial conditions are then obtained by multiplying rate constants with the in-situ concentrations of $NH_4^+$ or $NO_3^-$.

## 3.4. USE OF EXISTING DATABASES FOR THE SPECIFIC STUDY OF N SPECIATION IN THE SBNS AND DUTCH COASTAL WATERS

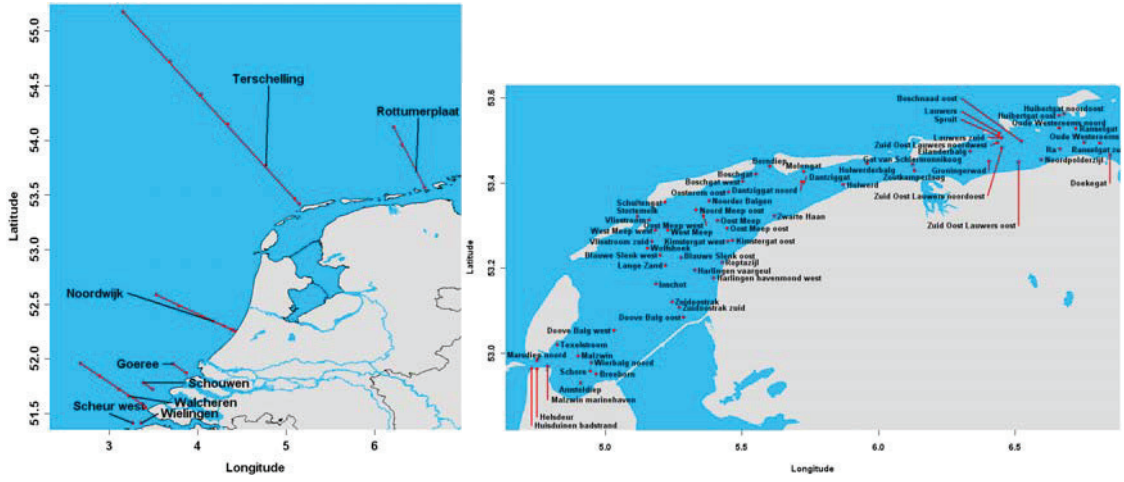


Fig. 2. Map of the Dutch coastal zone and Wadden Sea with sampling locations (●) at different transects.

Dissolved organic nitrogen data, together with the other nitrogen compounds (total nitrogen, dissolved nitrogen, particulate nitrogen, nitrate, nitrite a and ammonium) and associated parameters (e.g. salinity, suspended matter, dissolved and particulate organic carbon, phosphorus compounds and chlorophyll) have been used from the CANOPY database and combined with other available data from the North Sea and associated estuaries and rivers. The main data source was the DONAR database (35 years of data), managed by Rijkswaterstaat (www.waterbase.nl). This dataset was compared with measurement data from the database of the NIOO-CEME institute in Yerseke (The Netherlands) to assess the data quality and exclude artefacts due to changes in measurement techniques, human error, etc. Stations included in the DONAR data base are presented in figure 2.

Statistical analysis were performed with Statistica 7.0 (Statsoft) and R (R Development Core Team, 2006). Geographical illustrations were produced with GRASS 6.0 (Grass Development Team, 2006) and the maptools library of R (Lewin-Koh et al., 2005). Regression calculations were performed according to Venables & Ripley (2003), Koenker (2006) and Pinheiro et al. (2006).

Different water systems were distinguished to analyse the data: the Dutch Continental Shelf (further subdivided in a coastal zone and the open sea, the Wadden Sea, Haringvliet and the rivers Maas, Lek, Waal and IJssel. No long-term time series of DON were available for the rivers.

# 4. RESULTS AND DISCUSSION

## 4.1. GENERAL TEMPERATURE AND SALINITY DISTRIBUTION IN THE SBNS

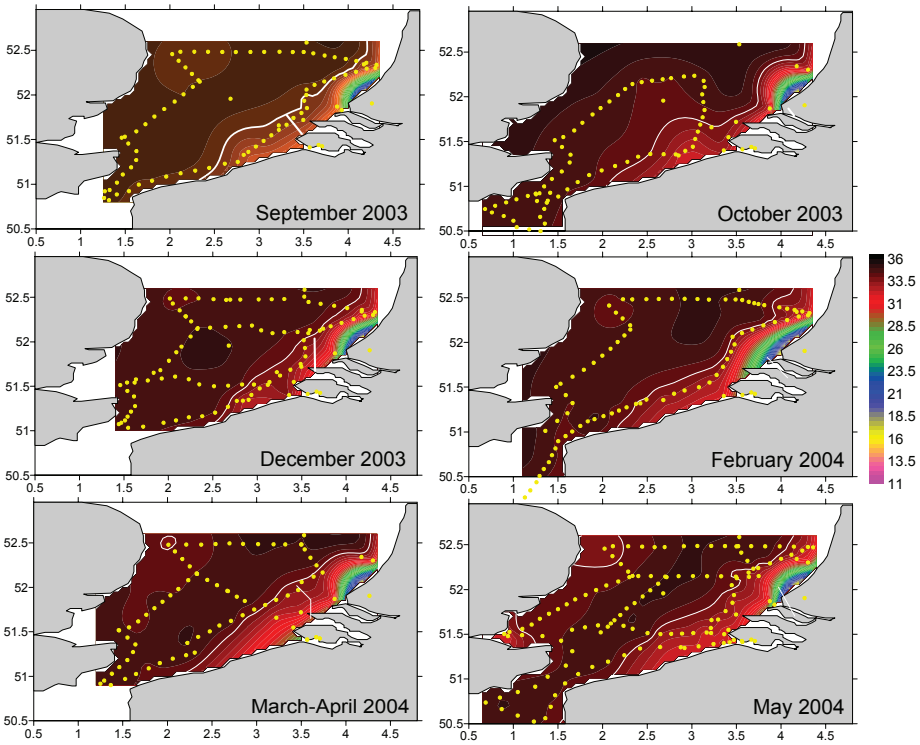


Fig. 3: Surface maps of salinity (PSU) during the 6 cruises (September 2003-May 2004) in the SBNS. Dots represent the sampling positions. Isolines correspond to salinity 34 (PSU). The isolines were computed after interpolation with the Krigging method using the SURFER software (Golden-Software).

Water temperature was homogenous over the whole water column and the averages for the 7 cruises were 19, 13, 10, 6.5, 7, 12, and 16°C for September 2003, October 2003, December 2003, February 2004, March 2004, May 2004 and October 2004, respectively.

The surface salinity distribution in the SBNS (Fig. 3) shows the presence of the river plumes of the Scheldt and Rhine (between 16.0 and 34.0 PSU) along the western coast extending until the northern boundary of the studied area. The plume of the Thames covered only a limited portion of the studied area and was only discernable close to the Thames river mouth (May 2004). The central part was rather homogeneous in its surface salinity distribution, with salinities ranging from 34.5 to 35.1 PSU.

## 4.2. CHLOROPHYLL A

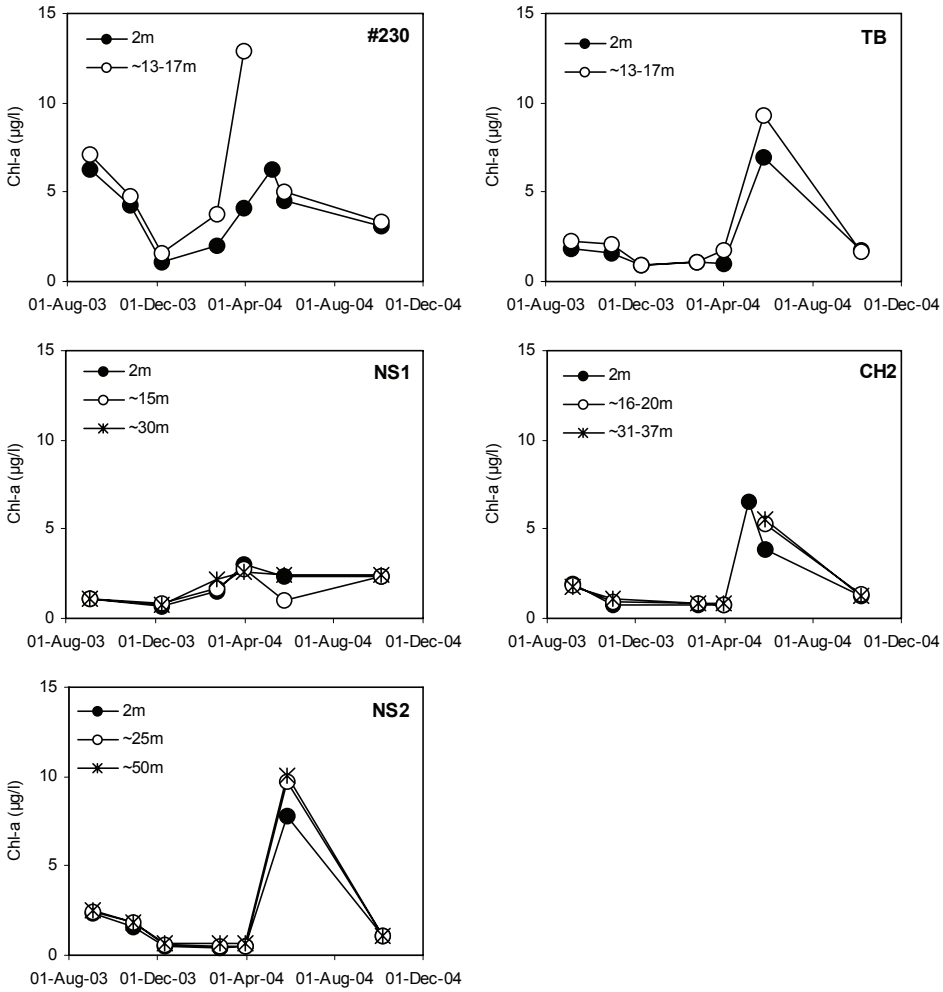


Figure 4. Seasonal trend in the chlorophyll a concentrations at different water depths at the fixed stations 230, NS1, NS2, TB and CH2.

The same seasonal distribution in chlorophyll a concentration (Fig. 4) was observed at the stations NS2, TB and CH2: a decrease between September and December 2003, low values in winter and a peak concentration in late May 2004. This pattern shows the spring bloom in May and the presence of phytoplankton in late summer / autumn. At station NS1, we have probably missed the spring bloom; the maximal chlorophyll a value in March was relatively small and malformed Phaeocystis colonies were observed in late May. We additionally visited stations 230 and CH2 in late April/early May. The chlorophyll a data showed higher concentrations during this cruise. The chlorophyll a concentrations were very similar at different water depths, except at station 230 in March 2004, indicating a usually well-mixed water column.

## 4.3. GENERAL NUTRIENTS (N AND P) DISTRIBUTION AND SPECIATION IN THE SBNS

### 4.3.1. Inorganic N and P: spatial and seasonal variations

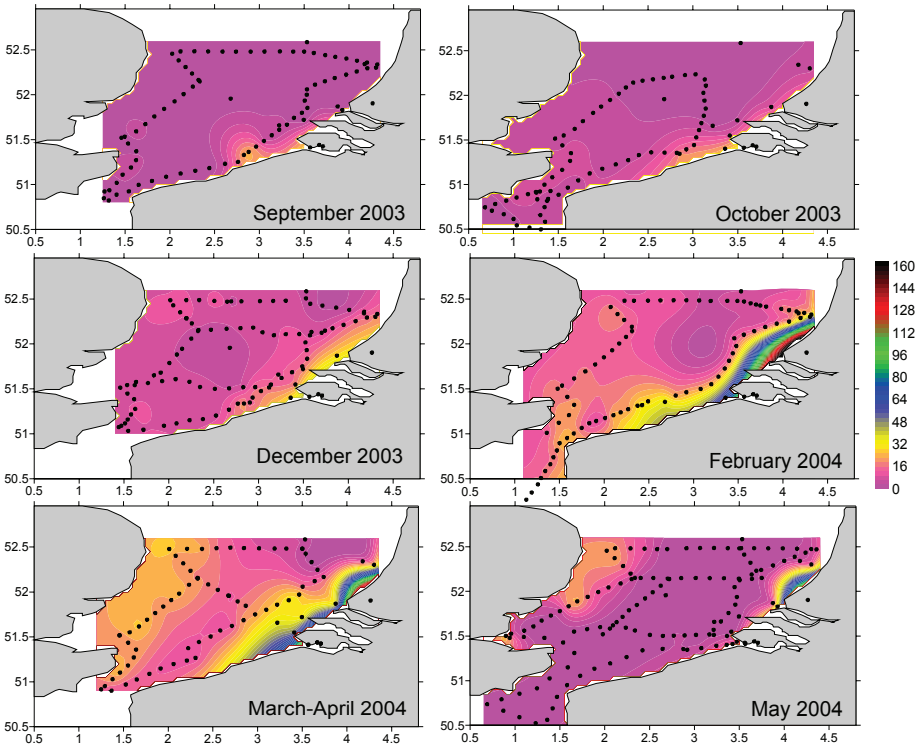


Fig 5: Nitrite + Nitrate (µM) distribution in the SBNS for the 6 cruises. Dots represent sampling positions. The isolines were computed after interpolation with the Krigging method using the SURFER software (Golden-Software).

Figures 5, 6 and 7 illustrate the spatial and temporal distribution of nitrate+nitrite (hereafter as nitrate or $NO_3^-$), ammonium and phosphate concentrations during the first six cruises in the SBNS (September 2003-May 2004).

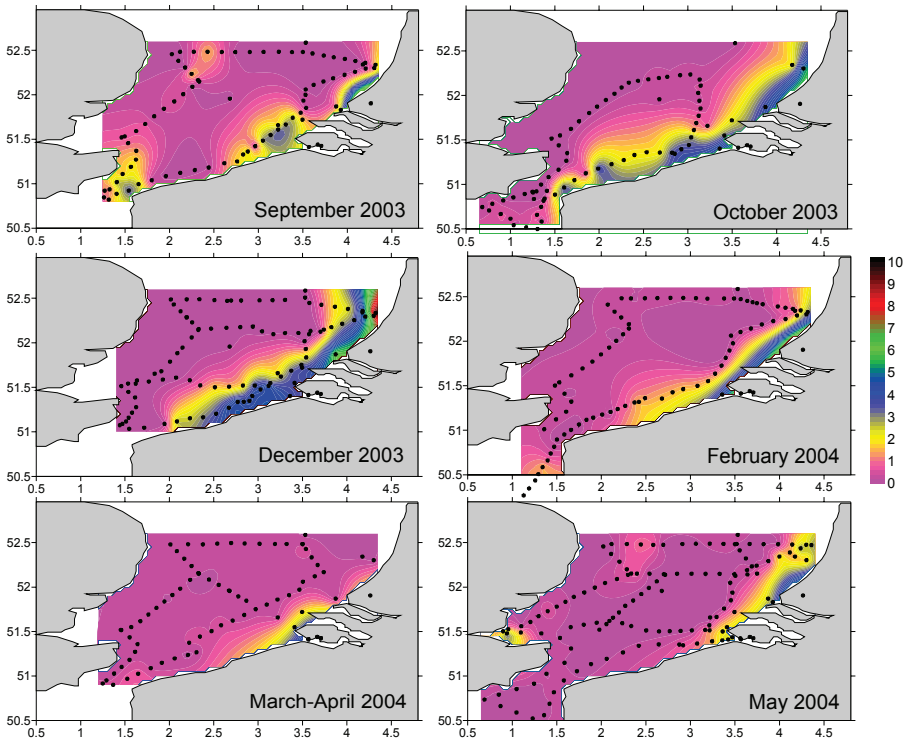


Fig 6: Ammonium (µM) distribution in the SBNS for the 6 cruises. Dots represent sampling positions. The isolines were computed after interpolation with the Krigging method using the SURFER software (Golden-Software).

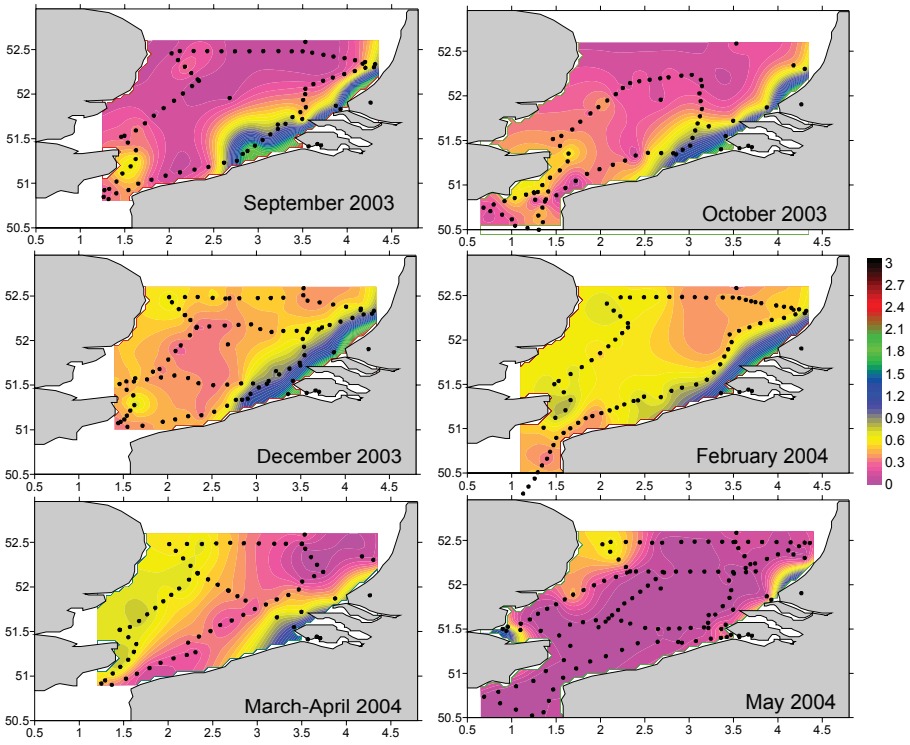


Fig 7: Phosphate (µM) distribution in the SBNS for the 6 cruises. Dots represent sampling positions. The isolines were computed after interpolation with the Krigging method using the SURFER software (Golden-Software).

In late summer (September 2003), the SBNS was completely depleted in DIN ($NH_4^+$ and $NO_3^-$) and $PO_4$, except in the direct neighborhood of the mouth of the Scheldt and Rhine estuaries. During fall-winter (from October to February), DIN concentrations increased, and the entire area was replenished with DIN and $PO_4$ by late February.

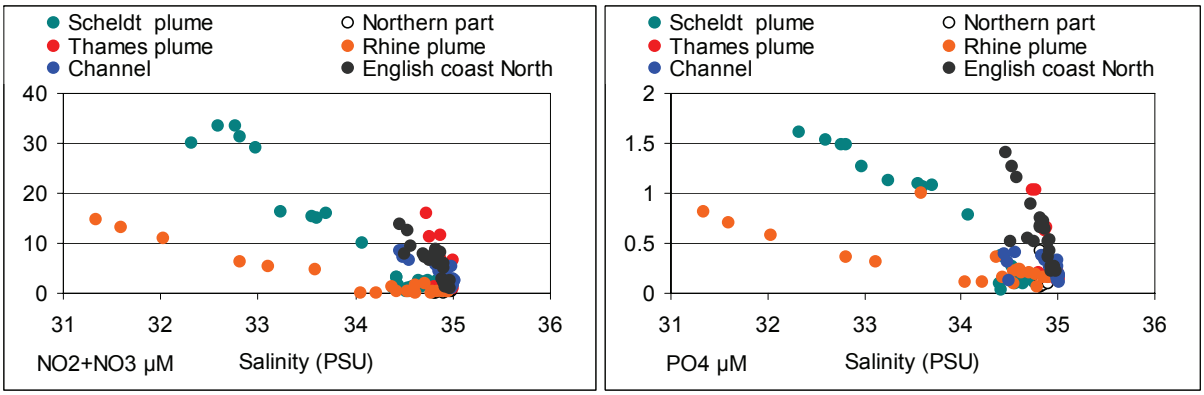


Fig.8. $NO_3^-$ and $PO_4^{\equiv}$ concentration as a function of salinity in the SBNS in October 2004

The influence of the Scheldt and Rhine riverine inputs was visible with the presence of a “plume” extending North and Southwards. Additionally, because of the different levels of $NO_3^-$ and $PO_4$ present in the Rhine and Scheldt estuaries, Rhine and Scheldt plumes can clearly be distinguished from $NO_3^-$ and $PO_4$ vs salinity plots (example Fig. 8). $NO_3^-$ and $PO_4$ were progressively distributed in the entire area and concentrations increased until February (for $PO_4$) or March-April (for $NO_3^-$). $NH_4^+$ was restricted to the river plumes area and increased until February. Between February and March-April (for $PO_4$ and $NH_4^+$) and between March-April and May (for $NO_3^-$), inorganic N and P nutrients decrease in the river plumes and the central part of the SBNS as a result of the spring phytoplankton bloom development.

Seasonal variations of $NH_4^+$, $NO_3^-$ and $PO_4$ can better be evaluated when considering the monthly averages (corresponding to all sampling periods) computed for both the Scheldt plume area and the central region of the SBNS (Fig. 9), based on high resolution N nutrients concentrations profiles (Figs 5, 6 and 7).

The global variation in DIN concentrations is tuned on the one side by the supply of DIN from external sources (estuarine, marine and atmospheric inputs) and on the other side by biological processes such as DIN uptake and regeneration processes occurring in both the benthic and pelagic compartments of the ecosystem; both of them being subject to seasonal variations.

In the Scheldt plume, average nitrate levels are relatively stable (between 10 and 20 µM) from September to December and increase to a maximum (50 µM) in late February. From February to May, they decrease regularly. In the central part, nitrate increases regularly from September (2 µM) to late March (17 µM), and decreases rapidly in May (3 µM). Ammonium concentrations in the Scheldt plume increase from

September to December and decrease from December to May. The central area of the SBNS was characterized by low $NH_4^+$ concentrations all year round, with a small and regular decrease between October and May. As a reduced and highly labile nitrogen compound, ammonium does not accumulate in the open sea part of the SBNS, but comprises a relatively small pool which probably cycles rapidly.

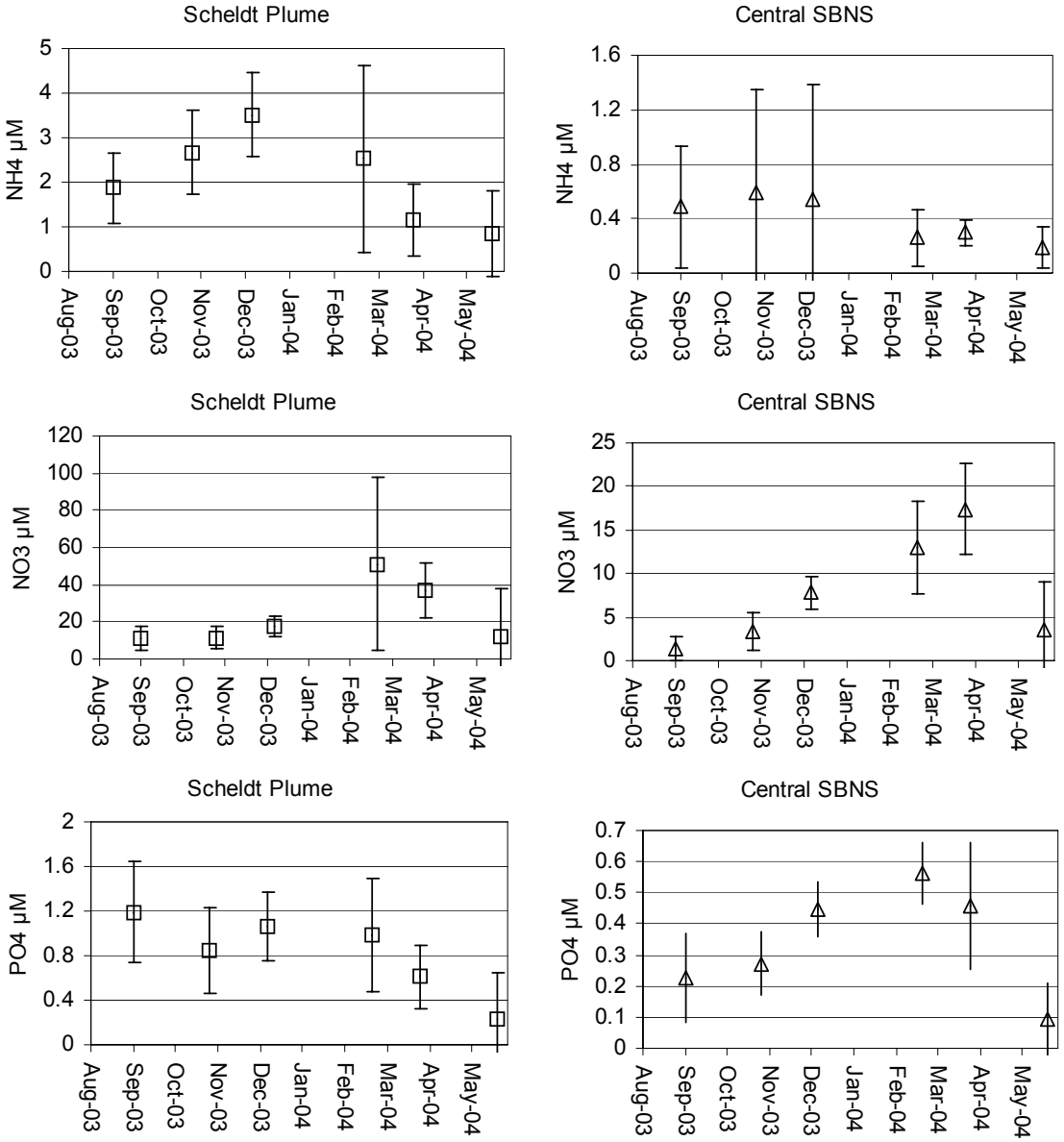


Figure 9: Average nitrate, ammonium and phosphate concentrations in the Scheldt plume and the central part of the SBNS. Error bars represent standard deviations on the averages calculated from the distributions shown in Figs 5, 6 and 7.

Phosphate concentrations in the Scheldt plume were relatively constant from September to late February and decrease from February to May. In the central part of the SBNS, $PO_4$ increase from September to end of February and decrease from February to May.

To conclude, lowest nutrient levels were recorded in May at the maximum of the phytoplankton biomass (see Fig. 4) and maximum in winter (December, February or March).

### 4.3.2. Organic N and P speciation in the SBNS

Organic N and P speciation were carried out at the 5 fixed stations and seasonal variations are shown in figures 10 and 11.
For nitrogen (Fig. 10), DON is the most abundant organic form except at station 230 located in the Scheldt Plume in spring. Organic nitrogen is in general highest in summer and fall and lowest in February (stations TB and CH2) or March (station 230, NS1 and NS2). The importance of the organic N pool compared to the inorganic one depends on the station. While the coastal station 230, located in the Scheldt plume region is dominated by inorganic N forms, the central waters have higher organic N content (Fig. 10).

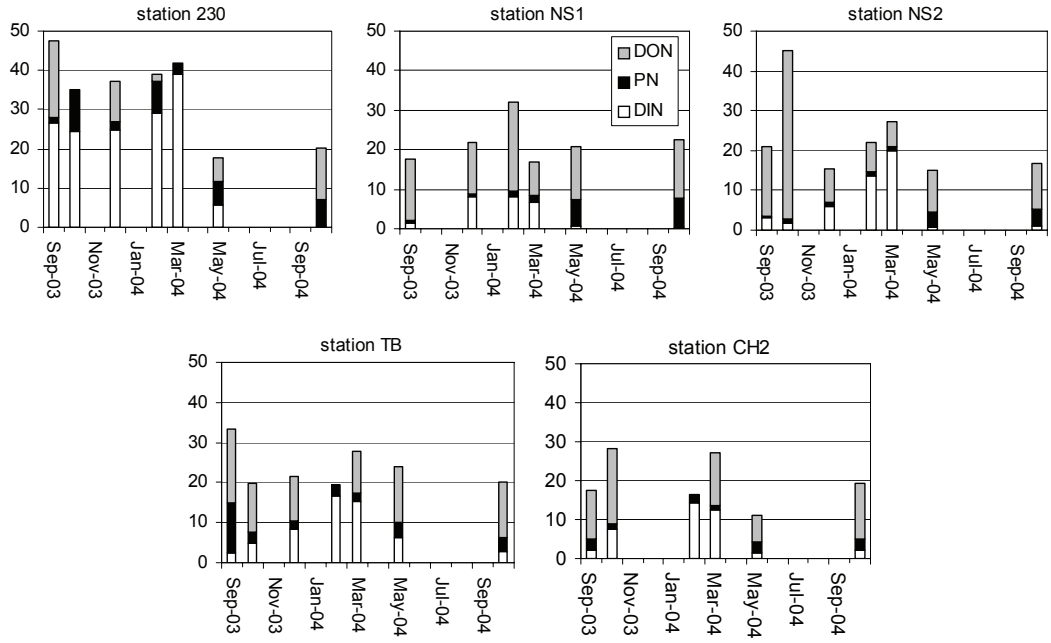


Fig. 10. Seasonal variations of inorganic (DIN) and organic N (Dissolved DON, and particulate PN) at the 5 process stations in the SBNS.

For phosphorus, polyphosphate is the least abundant P species (Fig. 11). The DOP concentration is elevated in late May and at some stations in September-October. In general, the seasonal trend in DOP seems to mirror that of phosphate. The seasonal trend in the POP concentration is obscured by variation in SPM load, particularly at the most turbid stations 230 and TB. The high POP value observed in February 2004 at CH2 is also due to a high SPM load.

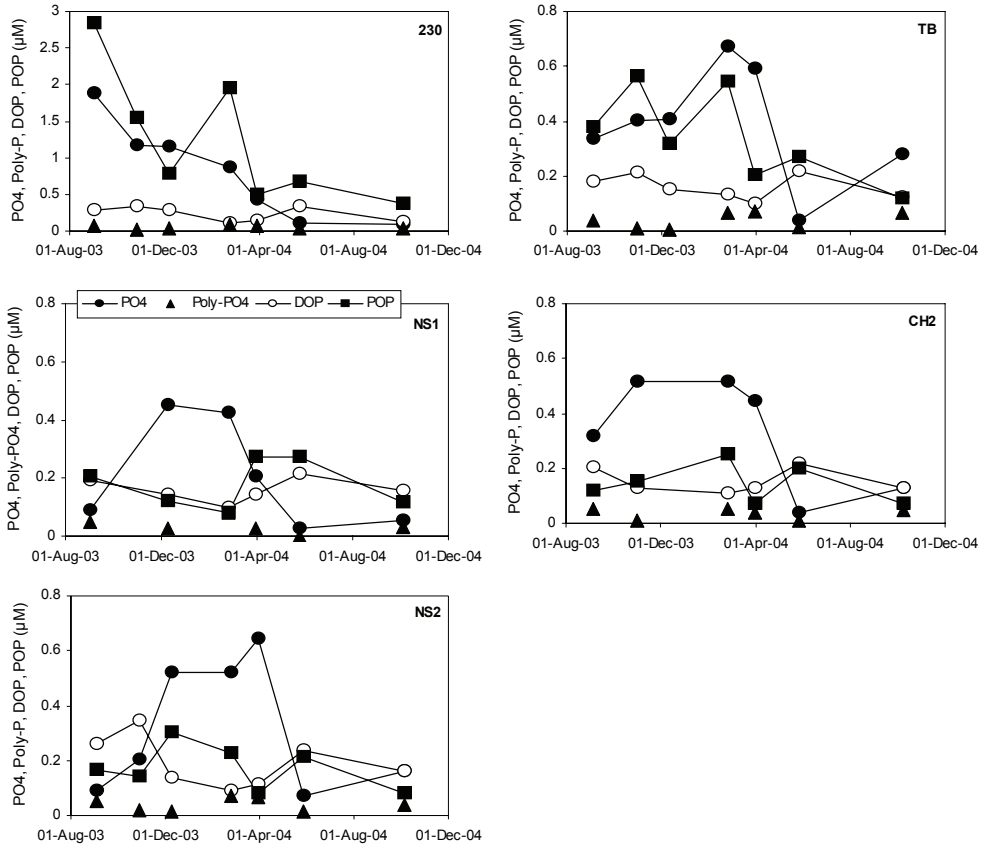


Figure 11. Seasonal trend in the depth-averaged phosphate, polyphosphate, DOP and POP concentrations at the fixed stations 230, NS1, NS2, TB and CH2.

### 4.3.3. DON distribution in the western coastal waters of the SBNS

Although the records of salinity and some other parameters in the DONAR data base are more than 35 years long, dissolved and particulate organic nitrogen have been determined routinely at various sampling locations on the Dutch Continental Shelf since 1991 (Fig. 12). For most of the locations the record is nowadays about fifteen years (Fig. 12) but for some minor records are on shorter periods (e.g. Walcheren 50).

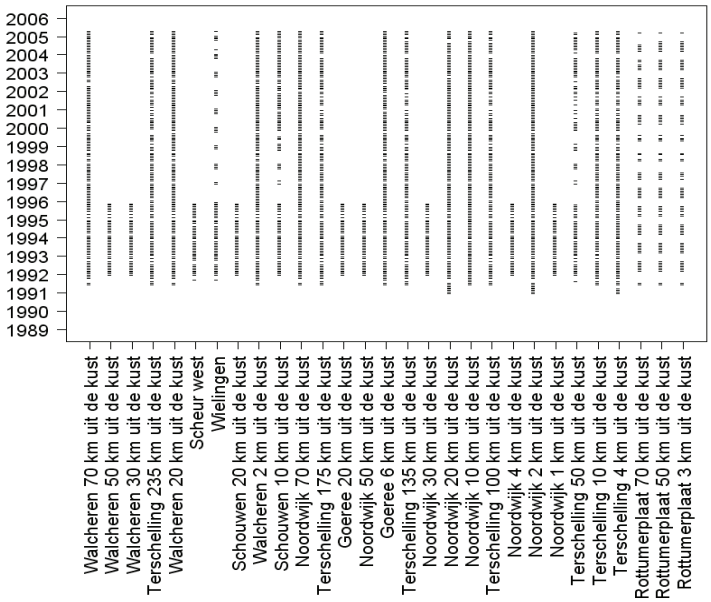


Figure 12. Spatial and temporal coverage of Dissolved Organic Nitrogen (DON) data in Dutch coastal zone (from Van Engeland, 2006)

Analysis of long-term trends showed that the concentration of DON significantly decreased between 1991 and 2005 (linear regression with log transformation) at all sampling locations in the Dutch coastal zone (Fig. 13), except at Rottumerplaat, going from 0.6 $\mu M.y^{-1}$ to 0.13 $\mu M.y^{-1}$.

Additionally, there is a seasonal signal in the DON concentration with lowest values in winter and highest early summer. The seasonal signal, however, was more pronounced in the coastal zone than in the open sea (Fig. 13).

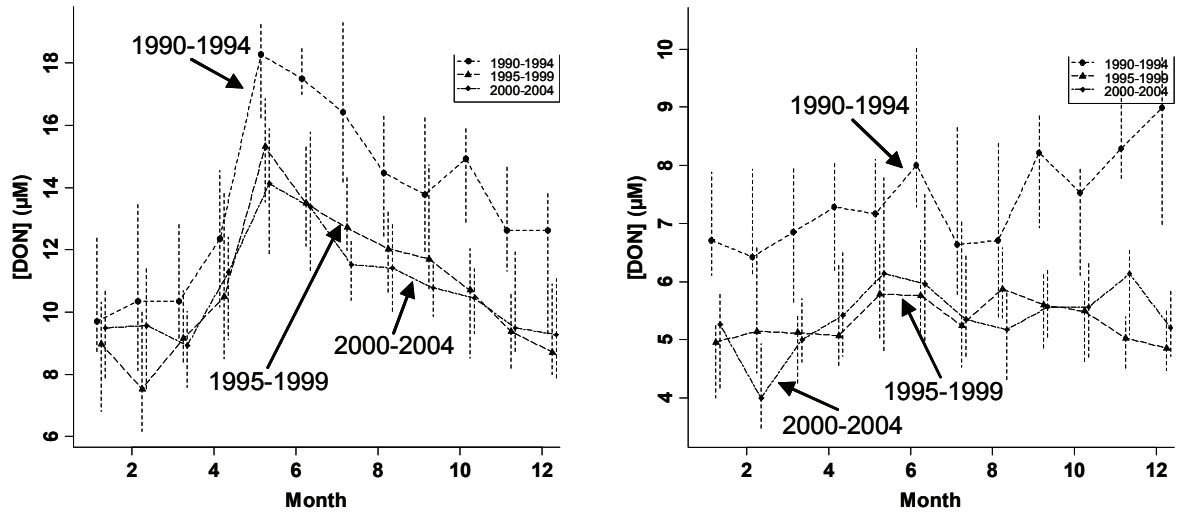


Figure 13. Seasonal evolution of the monthly median and interquartile range of the DON values for the coast (left) and open sea (right).

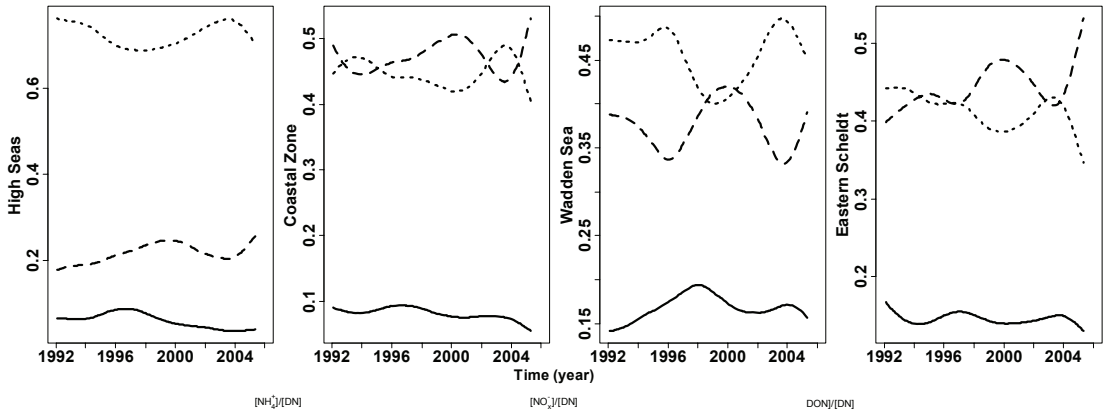


Figure 14. Year-to-year variation in the major fractions of dissolved nitrogen in the central area (S>30), the coastal zone, the Wadden Sea and the Oosterschelde. Ammonium (plain line), nitrate and nitrite (dashed line) and dissolved organic nitrogen (DON) (dotted line).

The contribution of DON to total dissolved nitrogen differs for the water systems studied (Fig. 14). In general, the DON concentration is a major constituent of dissolved nitrogen; highest ratios (>0.6) are found on the central area, decreasing to the coastal zone and Oosterschelde to ratios around 0.4. This is also reflected in the ratio of DON to total nitrogen for the Dutch coastal zone and central area during the years 1992-2004 (Fig. 15) and is in accordance with the measurements made in the SBNS stations during the CANOPY cruises (Fig. 10).

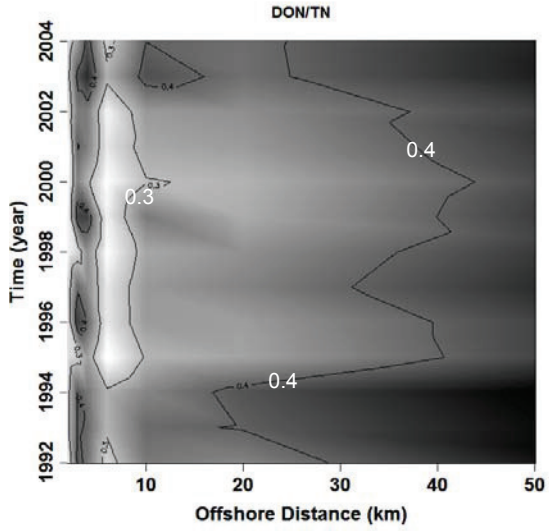


Figure 15. Temporal and spatial distribution of the ratio between Dissolved organic Nitrogen (DON, µM) and total nitrogen in the Dutch coastal zone and associated open sea.

## 4.4. PROCESSES OF N, P AND C TRANSFORMATION

### 4.4.1. Primary production

The depth integrated primary production was calculated using the photosynthetic parameters obtained from the P-E curve fit, the Chl *a* concentration (Fig. 4) and the light availability at each depth as described in methods. An example of P-E curves is presented in figure 16 for station 230. Additionally, respiration was not expected to be important in our production vs. irradiance incubations because DIC uptake was linear during at least a 12-hour period (Fig. 16).

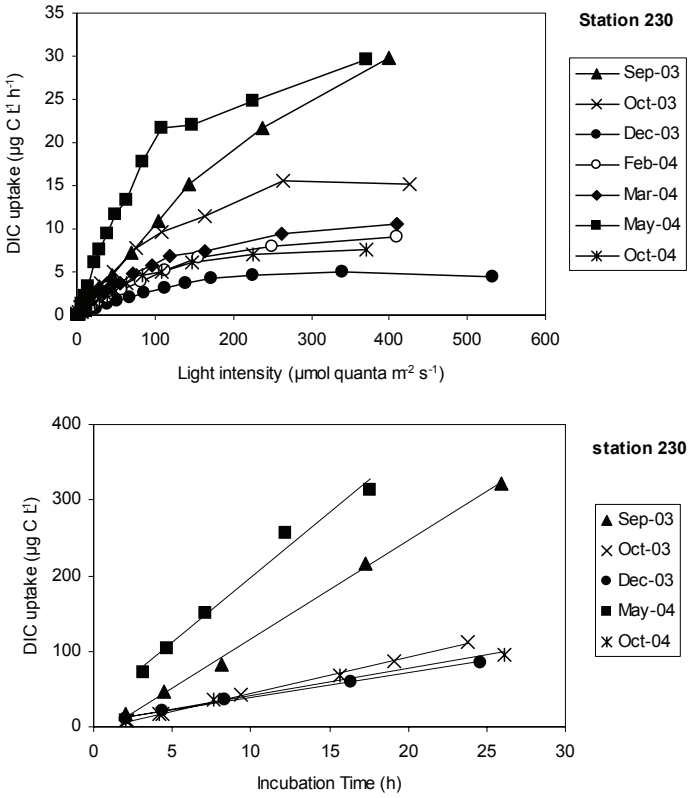


Figure 16. DIC uptake rates under variable light conditions (top) and as a function of time (bottom) at station 230.

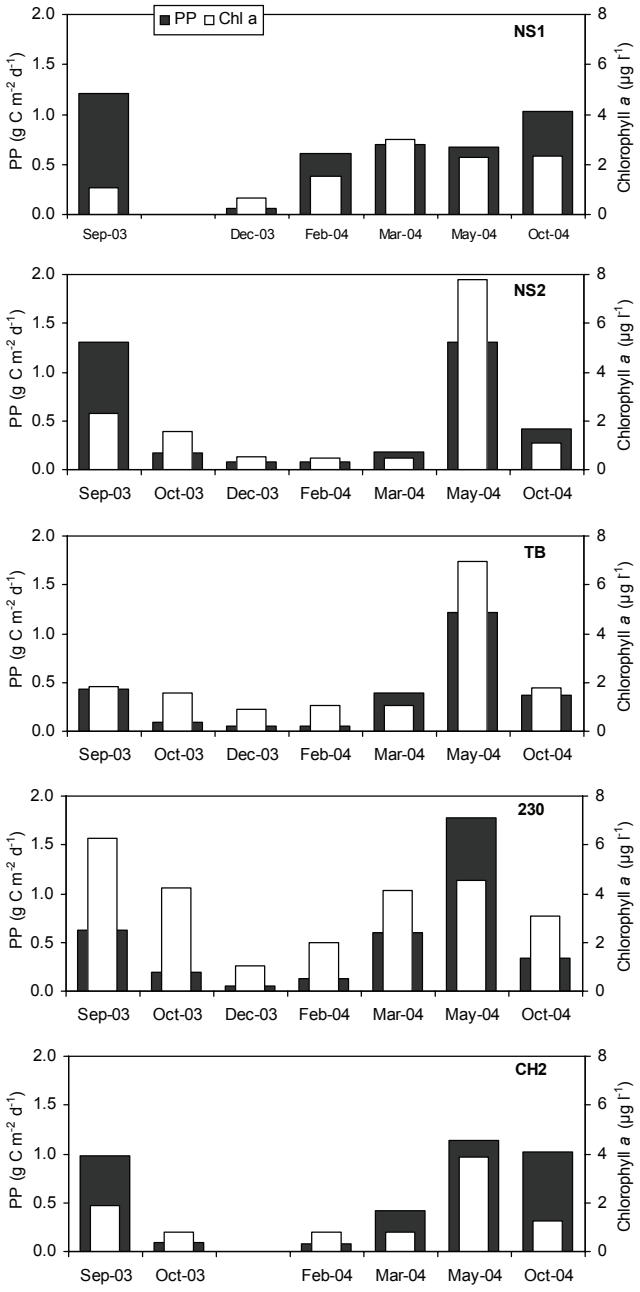


Figure 17. Depth integrated potential primary production (PP) and chlorophyll a concentrations (taken from van der Zee et al. a, subm.)

Primary production varied between 0.1 to 1.7 gC $m^{-2}$ $d^{-1}$. The temporal evolution was the same at stations NS2, TB, 230 and CH2: it decreased from September 2003 until December or February, after which it increased to reach a maximal value in May 2003 and declined again in October 2004 (Fig. 17). At station NS1, it was highest in September 2003. Primary production rates were of similar magnitude for the 5 stations.

### 4.4.2. Inorganic N uptake and regeneration processes in the water column of the SBNS

In the water column, DIN is taken up by microorganisms to produce organic material (OM) and, conversely, organic matter is mineralized by heteretrophic microorganism to recycle DIN.
Figure 18 illustrates the characteristic seasonal distributions of ammonium ($U_{NH4}$) and nitrate ($U_{NO3}$) uptake rates at the 5 process stations in the SBNS.

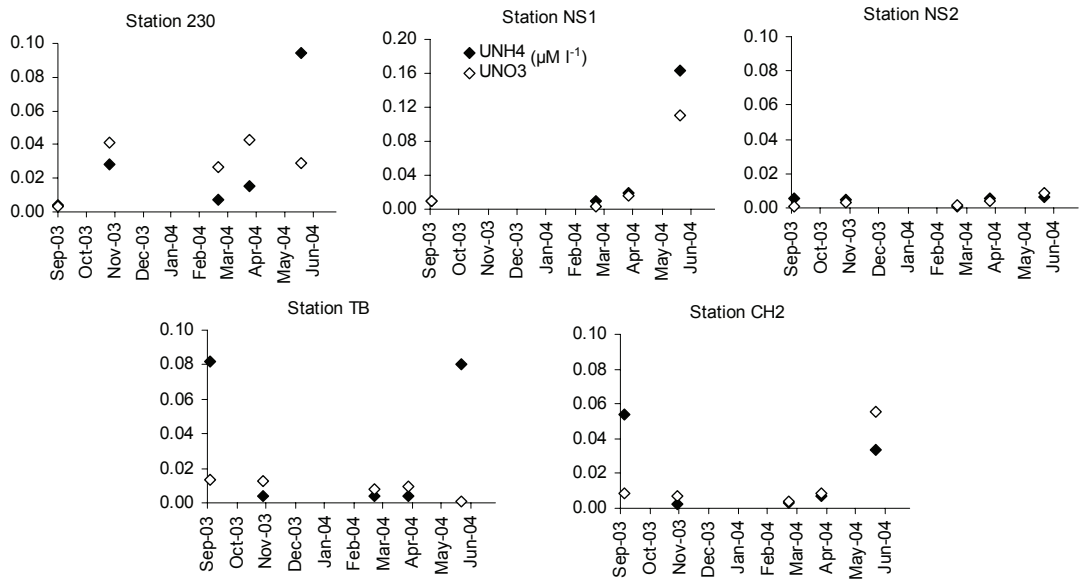


Figure 18: Ammonium (UNH4) and nitrate (UNO3) uptake rates (µM $h^{-1}$) at the 5 process stations in the SBNS for 5 cruises.

Between September 2003 and May 2004, $U_{NH4}$ and $U_{NO3}$ co-varied at all stations, except at stations 230 in May 2004, TB in September 2003 and May 2004 and CH2 in September 2003. Generally, $U_{NH4}$ varied from 0.001 and 0.16 µM $h^{-1}$, with maximum values recorded at the end of spring (all stations) and summer (stations CH2 and TB) phytoplankton blooms. Similarly, $U_{NO3}$ ranged from 0 and 0.11 µM $h^{-1}$, with peak values measured during the spring bloom (all stations, except station TB). At station NS2, $U_{NO3}$ maintained very low year round. In general the uptake of nitrate dominated in winter and spring and was lower in summer and fall (Fig. 19).

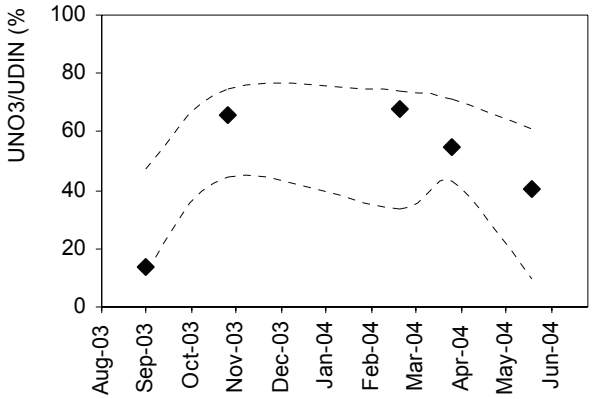


Figure 19: Contribution of nitrate to the total DIN uptake. Median (dots), percentile 10% and 90% (dotted line) values for the 5 incubation stations in the SBNS for 5 cruises.

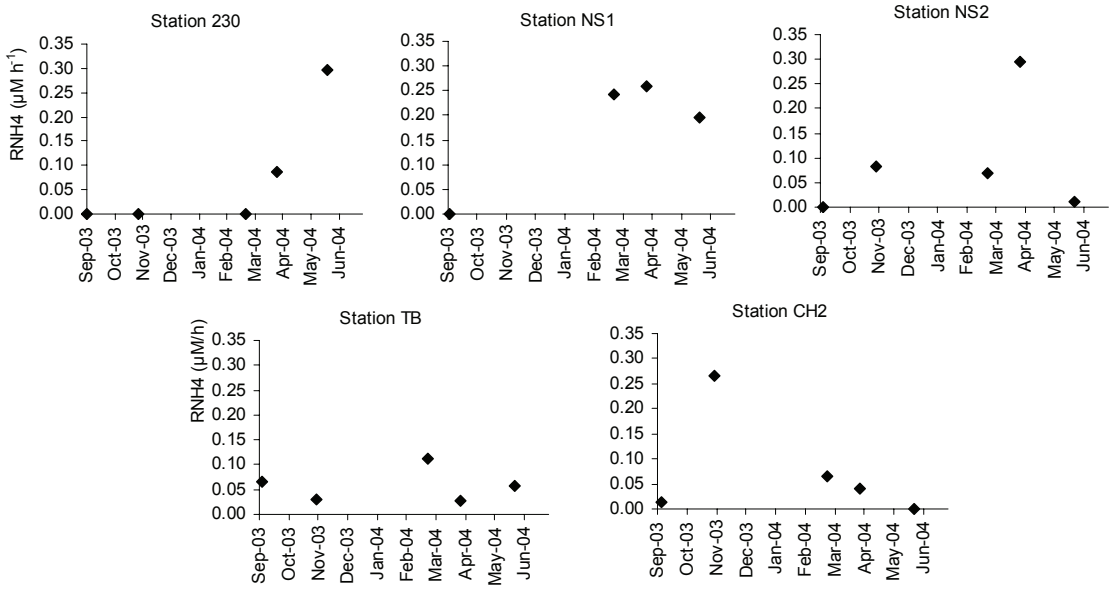


Figure 20: Ammonium regeneration rates (µM $h^{-1}$) measured at the 5 incubation stations in the SBNS, during the 5 cruises

Generally, at all stations, ammonium regeneration rates ($R_{NH4}$) varied between 0 and 0.30 µM $h^{-1}$ (Fig. 20). At stations 230, NS1 and NS2, $R_{NH4}$ maintained at low levels (< 0.1 µM $h^{-1}$) between September 2003 and February 2004 (except one high value at station NS1 in February), but attained maximum values during the spring phytoplankton bloom (in April 2004 for stations NS1, NS2 and May 2004 for station 230). At station NS2, following the peak value recorded at the onset of the spring bloom (April 2004), $R_{NH4}$ dropped to its minimum in late May 2004. Throughout the sampling period (September 2003-May 2004), station TB showed no significant seasonal differences in the means of $R_{NH4}$, which maintained low year round. At station CH2, the minimum $R_{NH4}$ recorded in late September 2003 was followed by a significant increase to a maximum value in October 2003. During fall-winter and

spring bloom period, $R_{NH4}$ dropped significantly, attaining again a minimum in late May 2004.

We can define the net pelagic DIN cycling regime (R-U) as $R_{NH4}$-$U_{DIN}$, where $U_{DIN}$ = $U_{NO3}$ + $U_{NH4}$. In this view, the water column of the SBNS can be considered as an U-dominant system (DIN-Uptake processes dominant) when (R-U) < 0 and as a R-dominant system (DIN-Regenerating processes dominant) when (R-U) > 0, respectively. Figure 21 illustrates the time course of the R-U at each of the sampling stations. It is noted that those stations for which |R-U| < 0.05 μM $h^{-1}$ were considered close to balance (R ≅ U).

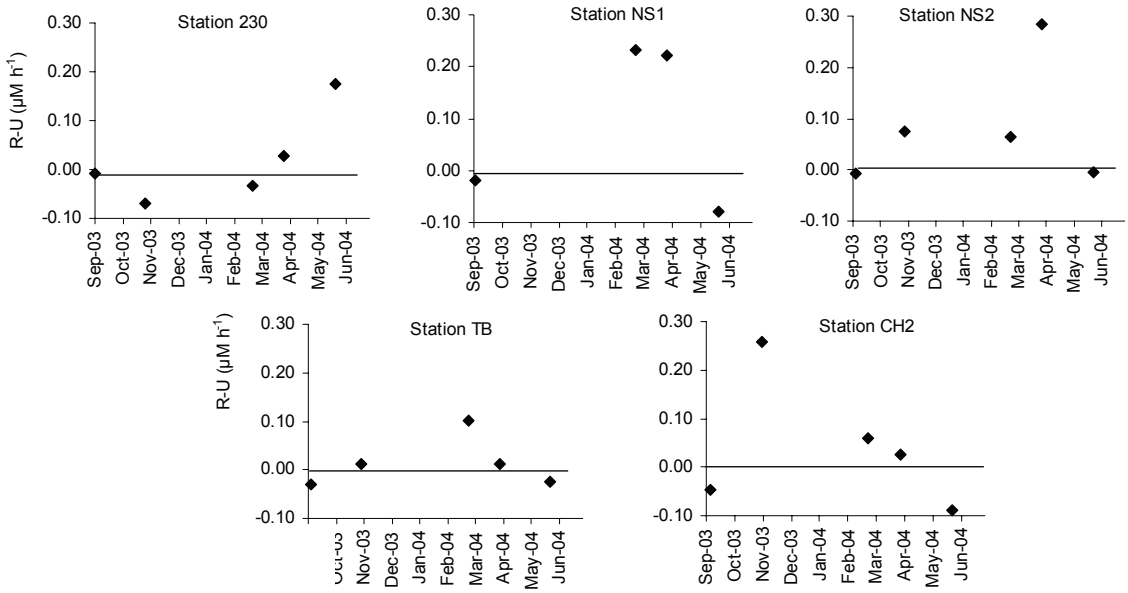


Figure 21: The DIN cycling regime in the water column of the SBNS (SBNS as U or R-dominant system).

At the stations located in the central area (northern part) of the SBNS (stations NS1 and NS2), the R-U values recorded during late summer (September 2003) were close to 0. Consequently, this pelagic system was close to balance. In winter, both station displayed positive R-U with a slightly regenerating pelagic system until February 2004 for station NS2 and a highly R-dominant pelagic system at station NS1 in February. During the spring phytoplankton bloom, this system varied from highly R-dominant in March 2004 (both stations) to slightly U-dominant (station NS1) and balanced (station NS2), respectively, in May 2004.

In the more southern part of the SBNS, close to the English coast (station TB), R-U was close to zero throughout the end of summer-fall period (September- October 2003) and attained a peak value (0.1 μM $h^{-1}$) at the end of winter (February 2004). Consequently, during this period, the pelagic system changed from balanced to highly R-dominant. During the spring phytoplankton bloom (April- May 2004), the R-U

values maintained close to zero and, thus, the SBNS system was in a balanced state. During late summer-winter period, the R-U measured at the station located in the English Channel (station CH2) varied from slightly U-dominant in September 2003 to R-dominant in February 2004. However, a peak R-U value was observed in late October 2003, when the pelagic system became highly regenerating. During the spring phytoplankton bloom, the system varied from balanced in April 2004 to slightly U-dominant in May 2004.
During late summer-winter period (September 2003-February 2004), the pelagic Scheldt plume system (station 230) was close to balance, except in October 2003 when it became slightly U-dominant. Also, the onset of the spring phytoplankton bloom (April 2004) was characterized close to balance (R ≅ U). This situation changed as the bloom progressed towards May 2004, when the water column of the Scheldt plume system turned into a highly R-dominant system (April-May 2004)

In general, the U dominance or R dominance of the pelagic system can be linked to the development of the phytoplankton population. Indeed, we can see that for stations NS1, NS2, CH2 and TB, R-U is related to the Chl-a concentrations (Fig. 22) : when chl-a > 2 µg/l, then R-U is negative and the system is net U dominant, while when the Chla < 2 µg/l, the system is clearly R dominant and the lower the Chla, the higher (R-U). The same relation was not found at station 230 possibly because this station, located in the Scheldt river plume, has important allochtonous organic material inputs enhancing regeneration processes even during phytoplankton blooms.

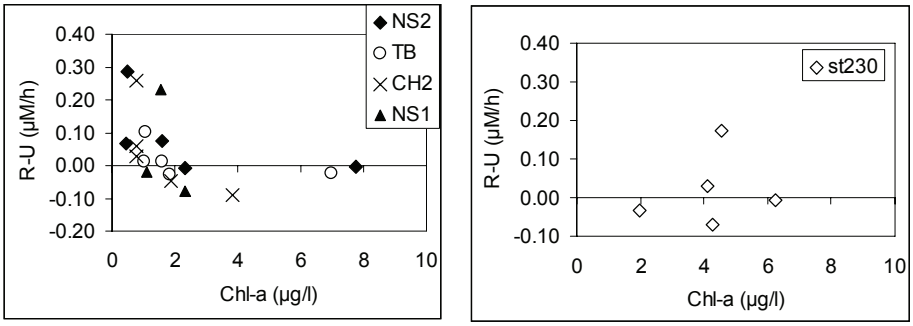


Figure 22 The net pelagic DIN cycling regime (R-U) as a function of the Chla concentration for the 5 stations in the SBNS

To summarize, the surface waters of the central parts of the SBNS are slightly U-dominant (~autotrophic) or close to balance during periods of phytoplankton blooms, and clearly R-dominant (~heterotrophic) during periods of low phytoplankton biomass. The surface waters of the Scheldt plume are in general close to balance for most periods of the year except in May 2004 which was clearly U-dominant.

### 4.4.3. P processes

Regeneration supplies most of the P to the primary producers in the sea. In the SBNS, the oceanic/riverine inflow rates of $PO_4$ are insufficient to support their seasonal cycle and internal recycling is required (Prandle et al. 1997; van der Zee et al. a, subm.). The P metabolism is particularly dependent on the rapid regeneration of $PO_4$ as there is no biological P uptake process analogous to $N_2$ fixation. Enzymes such as AP or 5PN can cleave DOP compounds in order to liberate the -$PO_4$ moiety, which can subsequently be taken up by the cell.
The enzyme 5PN is very substrate specific as it recognizes the nucleotide moiety of the substrate (Ammerman & Azam 1985). The 5PN activity in the dissolved fraction (< 0.2 µm) and the killed control samples was similar and very low, suggesting no net "free" enzyme activity (data not shown). The hydrolytic 5PN activity in the particulate fractions did not exhibit a seasonal variation similar to the AP activity, except at station 230 (Fig. 23).

The highest rates were found in September 2003 and May 2004 at this station. 5PN activity is generally contributed to bacteria (Ammerman & Azam 1985, 1991a & b, Nausch et al. 2004). Figure 23 shows the 5PN activity in the particulate size fractions < 2 µm and > 2 µm and in the total particulate size fraction. Both bacteria (< 2 µm) and algae (> 2 µm) contributed to the overall 5PN activity at all stations visited in the SBNS, but the extent varied from station to station and from campaign to campaign. The ATP hydrolysis rate ranged from 0 to 8.9 % $h^{-1}$ in the fraction < 2 µm, from 0.2 to 14 % $h^{-1}$ in the fraction > 2 µm and from 1.1 to 17.9 % $h^{-1}$ in the total particulate fraction.

The hydrolytic activity of 5PN may supply growing bacteria with nucleosides. For the regeneration of $PO_4$ is it important to know how much of the liberated $PO_4$ is assimilated by the algal or bacterial cell.

Figure 24 shows the percent uptake of $^{32}PO_4$ liberated by 5PN. It was usually larger in the fraction >2 µm, up to 96%, than in the smaller fraction, up to 42%. The coupled uptake in the larger size fraction also showed a clear temporal variation with the highest percentage uptake in May 2004, except for station NS2. Thus, phytoplankton did indeed use 5PN to provide the cell with $PO_4$, when the ambient concentrations were low in the SBNS. The smaller size fraction did not show this seasonal trend at stations NS1, NS2 and TB, whereas it did at station 230 and CH2. This indicates that bacteria utilized 5PN to a lesser extent to obtain $PO_4$ than the algae. The percentage of total coupled uptake ranged between 7% and 64%.

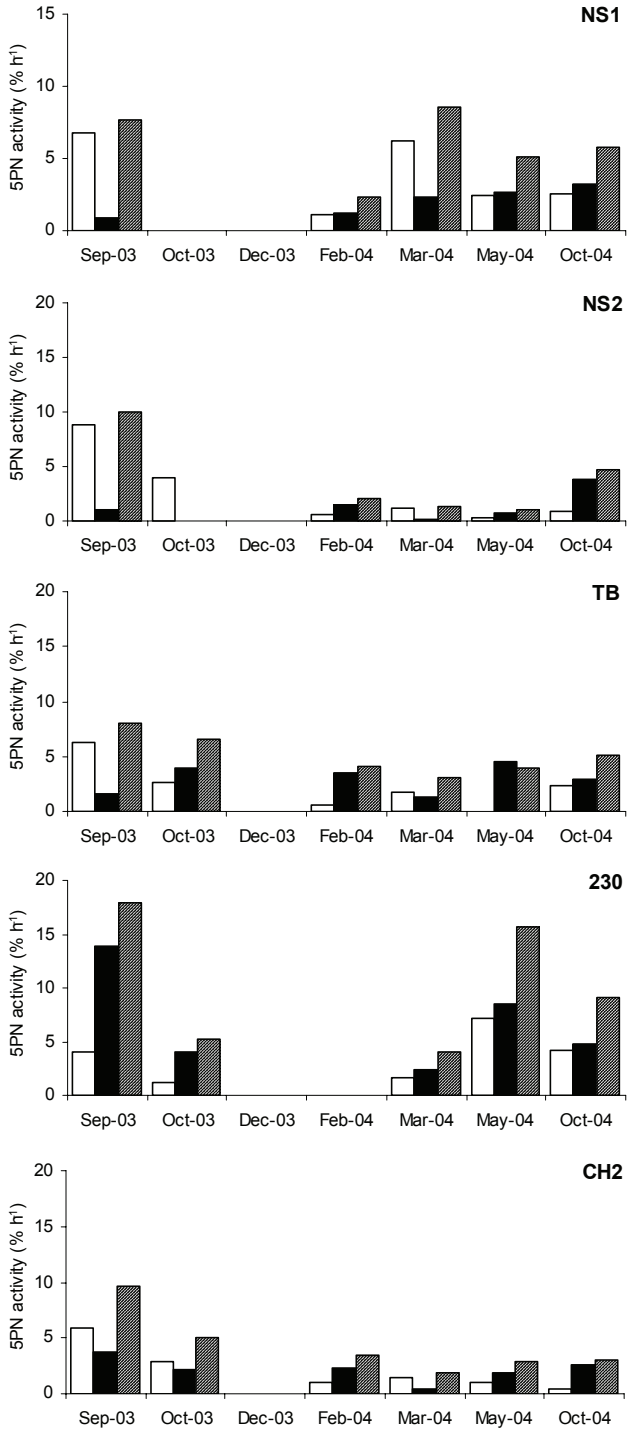


Figure 23 5PN activity in the < 2 µm, > 2 µm and the total particulate fraction (Taken from van der Zee et al.b, subm.)

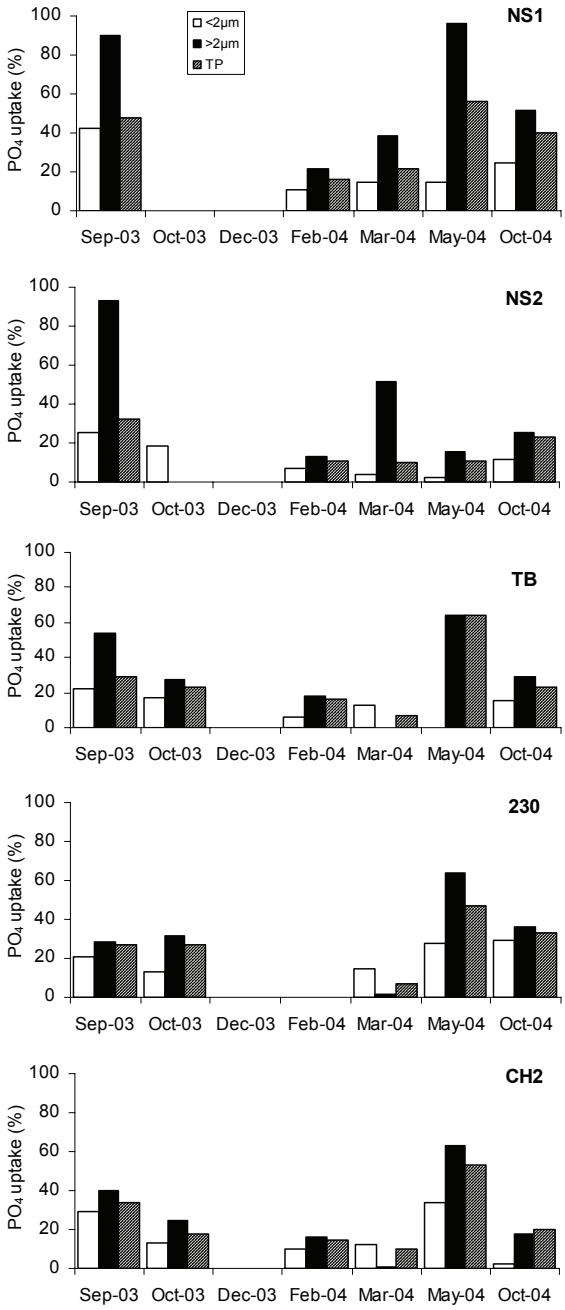


Figure 24 Percent coupled $^{32}PO_4$ uptake following $^{32}$P-ATP hydrolysis (Taken from van der Zee et al. b, subm.).

AP activity is commonly found in bacteria, phytoplankton as well as zooplankton both in the freshwater and the marine environment and hydrolyses a wide variety of organic P compounds due to its low specificity for the organic moiety (Jansson et al. 1988, Hoppe 2003). Figure 25 shows the AP activity at the 5 stations during the 7 campaigns. No AP activity was detected in the months October and December 2003 and February. The AP activity was very low in March 2004 and increased to maximum values in May 2004 Somewhat lower values were measured in September 2003 and October 2004. The maximal AP activity recorded using a substrate

concentration of 1 µM was 9 nM $h^{-1}$ in May 2004 at station NS1 (Fig. 25). The temporal trend in the AP activity resembles those of the $PO_4$ uptake rate and of the inverse of the $PO_4$ concentration. AP activity in the SBNS can be used as an indicator of P stress and regarded as an alternative pathway for the acquisition of $PO_4$.

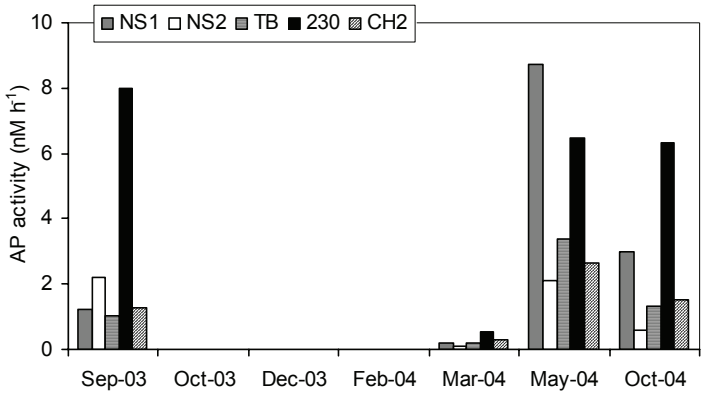


Figure 25 Alkaline phosphatase activity (Taken from van der Zee et al. b, subm.)

The kinetic experiments performed in May and October 2004 allowed us to estimate the maximum potential activity Vmax (Tab. 2). The highest $V_{max}$ was 20 nM $h^{-1}$ in May and 17 nM $h^{-1}$ in October 2004 (Tab. 2). Those values are within the range reported in literature (Hoppe 2003).

Table 2. $V_{max}$ estimated from the kinetic assay (modified from van der Zee et al. b, subm.)

| Station | May 2004 $V_{max}$ (nM $h^{-1}$) | October 2004 $V_{max}$ (nM $h^{-1}$) |
|---|---|---|
| NS1 | 20 | 6 |
| NS2 | 4 | 2 |
| TB | 7 | 5 |
| 230 | 8 | 17 |
| CH2 | 6 | 4 |

The biological $PO_4$ uptake rate measured with tracer addition of $^{33}PO_4$ was maximally 6 nM $h^{-1}$ in May 2004. The fluxes measured with the saturating substrate addition in the AP assay amounted to 15 nM $h^{-1}$. However, this value is an overestimation as the available substrate concentrations were much lower than 3 µM. In May and October 2004, lower MUF-$PO_4$ substrate concentrations were also used. In May 2004, the DOP concentrations were between 0.20 and 0.34 µM. However, not all DOP is necessarily biologically available. Between 11 and 65 % of the DOP in the Gironde plume waters were composed of easily hydrolysable compounds (Labry et al. 2005). Therefore, the AP activity at the lowest added substrate concentration (100 nM) was

compared with the $PO_4$ uptake rates (Tab. 3). The AP activity at 100 nM substrate concentration was higher than the $PO_4$ uptake rate at the stations 230 and NS2, while it was a substantial part of the $PO_4$ uptake rate at the other stations. In October 2004, the DOP concentrations were between 0.12 and 0.20 µM. The AP activity resulted in hydrolysis rates very similar to the $PO_4$ uptake rates, except at station TB (Tab. 3). Thus, regeneration of organic phosphorus was a quantitatively important process in the SBNS. The hydrolysis rates were higher than the inorganic P uptake rates when saturating concentrations of MUF-P were used in May and October 2004 (Tab. 2).

Table 3. Comparison of regenerated $PO_4$ fluxes and direct $PO_4$ uptake rates (Taken from van der Zee et al.b, subm.).

| | May 2004 | | | October 2004 | | |
|---|---|---|---|---|---|---|
| Station | AP[1] (nM $h^{-1}$) | 5PN[2] (nM $h^{-1}$) | $^{33}PO_4$ (nM $h^{-1}$) | AP[1] (nM $h^{-1}$) | 5PN[2] (nM $h^{-1}$) | $^{33}PO_4$ (nM $h^{-1}$) |
| NS1 | 2.4 | 0.1 - 5.1 | 5.8 | 0.6 | 0.1 - 5.8 | 0.7 |
| NS2 | 0.8 | 0.0 - 1.1 | 0.7 | 0.2 | 0.1 - 4.7 | 0.3 |
| TB | 0.8 | 0.1 - 3.9 | 3.9 | 0.3 | 0.1 - 5.1 | 1.1 |
| 230 | 2.7 | 0.3 – 16 | 2.1 | 0.9 | 0.2 - 9.1 | 1.1 |
| CH2 | 0.8 | 0.1 - 2.8 | 1.3 | 0.3 | 0.1 - 3.0 | 0.4 |

[1] Measured AP activity upon 100 nM MUF-$PO_4$ addition, [2] 5PN activity assuming an *in situ* nucleotide P concentration of 2 - 100 nM

The seasonal trend in the coupled $PO_4$ uptake indicates that the 5PN activity contributes to the regenerated P flux. Concentrations of total dissolved 5'-nucleotides were not measured, but a concentration of 2 nM of dissolved nucleotide P (Ammerman and Azam, 1991b) or even a higher availability of nucleotide P of 100 nM based on average dissolved DNA and RNA concentrations in coastal waters (Karl and Bailiff, 1989) could be assumed. In this case, the 5PN activity would liberate up to 16 nM $PO_4$ $h^{-1}$ (Tab. 3). The maximal 5PN activity in May 2004 is close to the measured $PO_4$ uptake rate at the stations NS1, NS2 and TB, while it is twice and almost 8 times the $PO_4$ uptake rate at CH2 and station 230, respectively. In October 2004, the maximal 5PN activity is 5 to 16 times the direct $PO_4$ uptake rate. The coupled uptake of hydrolysed $PO_4$ is, however, greater in May than in October 2004. Therefore, the flux of regenerated $PO_4$ is more likely to play a quantitatively important role in the P assimilation in May 2004. The AP activity at a substrate concentration of 100 nM and the direct $PO_4$ uptake rate are both within the range of potential regenerated $PO_4$ flux by 5PN. Hence, the regenerated P flux could be many times higher than the direct $PO_4$ uptake if suitable DOP compounds are available. But $PO_4$ is always the preferred substrate, when both $PO_4$ and various DOP compounds are available (Björkman and Karl, 1994).

## 4.5. $CO_2$ DYNAMICS AND AIR-SEA EXCHANGE

### 4.5.1. In the Scheldt Plume

Two data analysis approaches were applied to study the $pCO_2$ dynamics in the Scheldt plume. The first one is based on a high temporal dataset of $pCO_2$ (sampling frequency twice a week) at a fixed station (Zeebrugge station) that allows to highlight the relative importance of temperature change and biological activities involved in the seasonal $pCO_2$ dynamics. The second approach is a high spatial coverage of $pCO_2$ (the survey area approach, one to three surveys per month) that allows us to compute the air-sea $CO_2$ fluxes taking into account the strong spatial heterogeneity of the system.

Figure 26 shows the seasonal cycle of $pCO_2$ in surface seawaters at Zeebrugge station and from the survey area approach. The surface waters at Zeebrugge station show stronger $CO_2$ oversaturation with respect to the atmosphere than the whole Scheldt plume. The Zeebrugge station was characterized by rather low salinities (not shown), while the survey area approach values reflected the overall range of salinities (and mixing) in the Scheldt plume. Most of the time, profiles against salinity in the Scheldt plume are typical for estuarine environments, with $pCO_2$ increasing with decreasing salinities (data not shown). Hence, $pCO_2$ values at the Zeebrugge station tended to be higher than average values from the survey area approach. The range of $pCO_2$ values was similar from one year to another, with minimal values of around 100 µatm and maximal values of 600 and 900 µatm, for the survey area approach and Zeebrugge station, respectively. In 2003 and 2004, a stronger decrease of $pCO_2$ during the spring phytoplanktonic bloom was observed in comparison to 2001 and 2002.

The seasonal succession of phytoplanktonic blooms as described by Reid et al. (1990) and Rousseau et al. (2002), was apparent in the successive decreases of $pCO_2$ observed in 2003 (Fig. 26). The diatom bloom started in February, was followed by a mixed bloom of diatoms and *Phaeocystis* from March to May, and ended with a small diatom bloom in late August. The increase of $pCO_2$ values observed during summer was due to heterotrophic processes (see hereafter). The $pCO_2$ decrease in the whole plume occurred earlier than at station Zeebrugge. This was related to the onset of the spring phytoplanktonic bloom in the offshore coastal waters, due to higher light penetration in the water column (Borges and Frankignoulle, 1999, 2002; van der Zee and Chou, 2005).

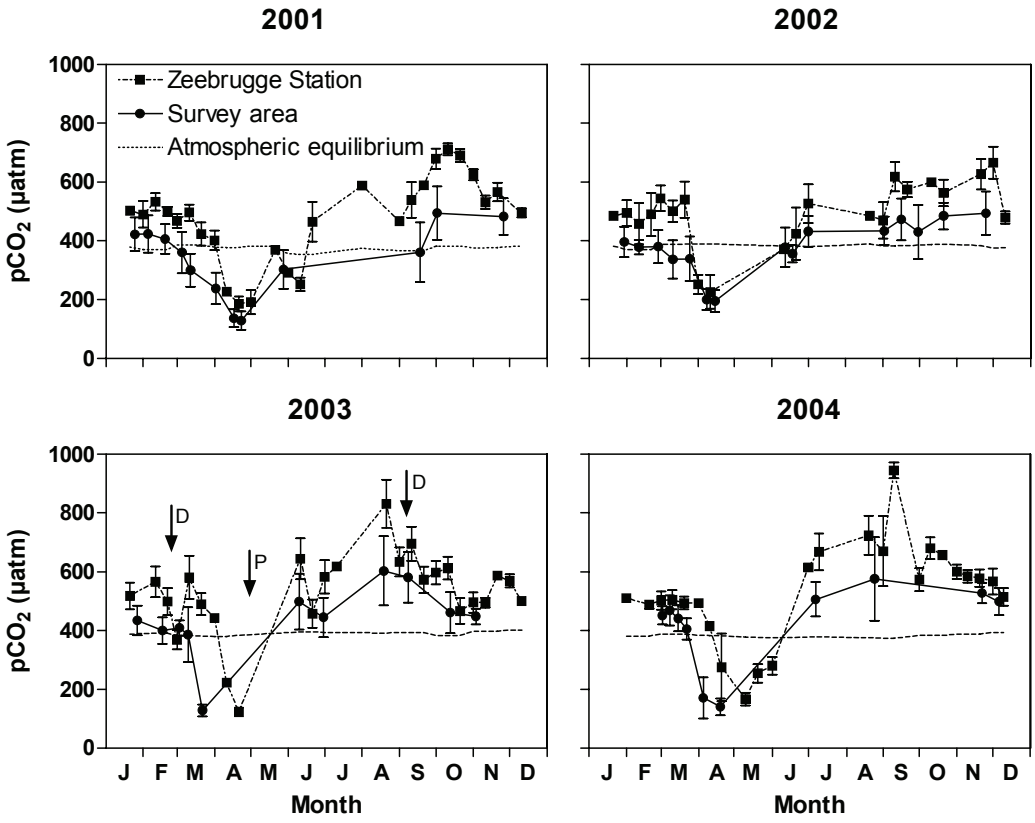


Figure 26. Averaged $pCO_2$ (µatm) on surface waters of the Scheldt plume (survey approach; blue circles) and at Zeebrugge station (red squares) from 2001 to 2004. Data are mean ± standard deviation (SD). The dotted line represents atmospheric $pCO_2$. P and D refer to *Phaeocystis sp.* and diatoms, respectively. Adapted from Schiettecatte et al. (2006).

Figure 27 shows the air-sea $CO_2$ fluxes computed for the Scheldt plume, from 2001 to 2004, from the survey area and Zeebrugge station. The air-sea $CO_2$ fluxes computed at the Zeebrugge station were, most of the time, one order of magnitude higher than those computed from the survey area approach. This is related to the higher $pCO_2$ values at the Zeebrugge station as discussed above. For instance, both approaches showed that in 2002 the Scheldt plume was on average a net source of $CO_2$ to the atmosphere of 19 (± 4) and 2 (± 3.1) mmol C $m^{-2}$ $d^{-1}$ for, respectively, Zeebrugge station and survey area approaches. A sink of atmospheric $CO_2$ was only observed during the spring phytoplanktonic bloom for the area survey and Zeebrugge station approaches (up to -40 mmol C $m^{-2}$ $d^{-1}$). During the rest of the year, surface waters were a source of $CO_2$ to the atmosphere, even during the late summer bloom. Strong wind speed short term events (up to 20 m $s^{-1}$) were also responsible for high air-sea $CO_2$ fluxes, up to 22 mmol C $m^{-2}$ $d^{-1}$ for the survey area approach (referred to as $U_{10}$ on Fig. 27). Other events could be responsible for extreme air-sea $CO_2$ flux values at the Zeebrugge station, such as the presence of lower salinity with higher $pCO_2$ water mass and/or remineralization of resuspended organic matter (referred as

S and DIC on Fig. 27). These processes could be directly associated to storm events, although the presence of lower salinity waters was also dependent on the overall wind speed direction.

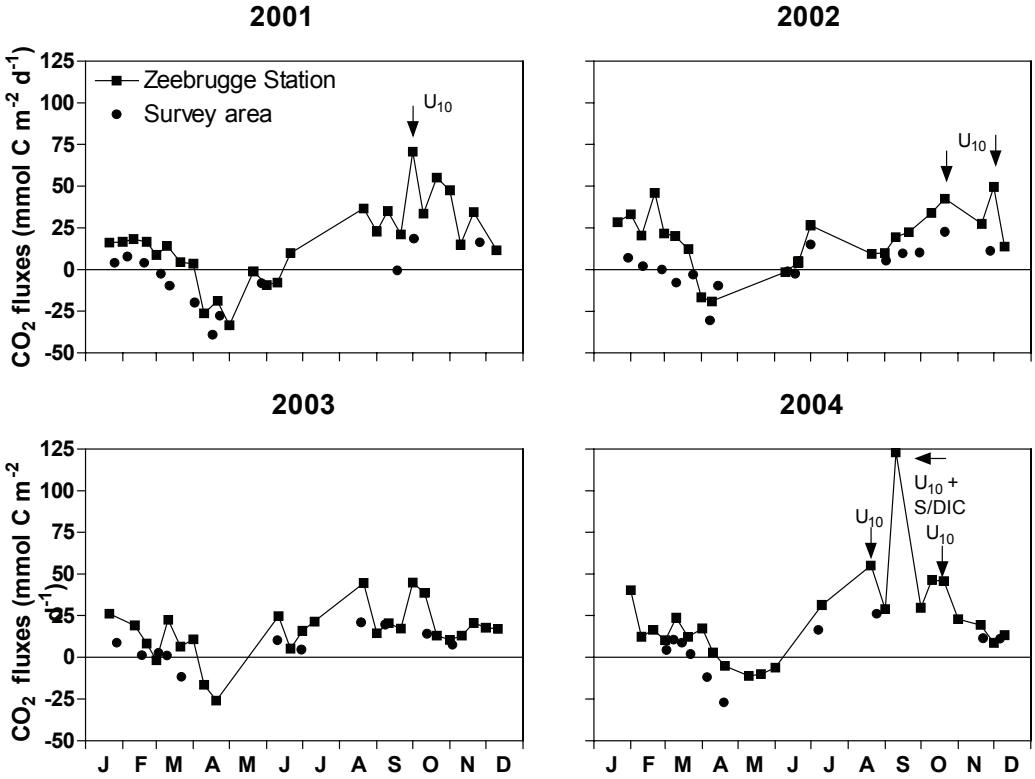


Figure 27. Air-sea $CO_2$ (mmol C $m^{-2}$ $d^{-1}$) fluxes from spatially integrated data (survey area approach; blue circles) and at Zeebrugge station (red squares) from 2001 to 2004. For air-sea $CO_2$ fluxes computation, the gas transfer velocity parameterization as a function of wind speed given by Nightingale et al. [2000] and wind speed data from station Vlakte van de Raan were used. $U_{10}$ refers to strong wind speed events, S to an observed decrease of salinity, and DIC to inputs of dissolved inorganic carbon from the sediments. Adapted from Schiettecatte et al. (2006).

Table 4 shows annually integrated air-sea $CO_2$ fluxes based on the survey area approach. Based on results from 2002, which was the year with the best temporal coverage, the plume of the Scheldt acted as a net source of $CO_2$ to the atmosphere of 0.7 ($\pm$ 1.1) mol C $m^{-2}$ $yr^{-1}$ (N&al). In 2001, the plume of the Scheldt would have been a sink for atmospheric $CO_2$ (-1.7 $\pm$ 1.8 mol C $m^{-2}$ $yr^{-1}$; N&al). As shown on Figure 26, there was a lack of data in 2001 during summer, when surface waters showed during the other years the highest $CO_2$ oversaturation and consequently high $CO_2$ emissions to the atmosphere. In 2003 and 2004, $CO_2$ fluxes were higher than in 2002, respectively (2.6 $\pm$ 1.1 and 1.9 $\pm$ 1.7 mol C $m^{-2}$ $yr^{-1}$). A. In 2003 and 2004, the lack of data during the spring phytoplanktonic bloom led to the overestimation of the annually integrated air-sea $CO_2$ flux. This clearly highlights the need of high temporal data coverage for studies of DIC dynamics in coastal environments.

The annually integrated air-sea $CO_2$ fluxes we computed in this study for year 2002 are about 50% lower than of those computed by Borges and Frankignoulle (2002) (Tab. 4). These authors estimated annual air-sea $CO_2$ areal fluxes from a composite annual cycle based on campaigns carried out over 4 years (1996 to 1999). This approach probably biased the air-sea $CO_2$ fluxes, since the annual average $\Delta pCO_2$ value of Borges and Frankignoulle (2002) is more than two times higher than the one we obtained for 2002, 16 and 7 µatm, respectively.

Table 4. Annually integrated air-sea $CO_2$ fluxes (mol C $m^{-2}$ $yr^{-1}$) in the Scheldt plume computed using surface water $pCO_2$ data acquired during the survey area, the gas transfer velocity parameterizations as a function of wind speed given by Liss and Merlivat (1986; L&M), Wanninkhof (1992; W), Wanninkhof and McGillis (1999; W&McG) and Nightingale et al. (2000; N&al), and wind speed data from station Vlakte van de Raan. Numbers in parenthesis indicate standard errors of the computed fluxes. Annually integrated $CO_2$ emissions from the Scheldt plume were estimated from these computed fluxes and estimated surface areas of the plume during each survey (based on the distribution of salinity). These $CO_2$ emissions are compared to the ones calculated by Frankignoulle et al. (1998) and Gazeau et al. (2005) in the inner Scheldt estuary. Adapted from Schiettecatte et al. (2006).

| **Fluxes (mol C $m^{-2}$ $yr^{-1}$)** | **Year** | **L&M** | **W** | **W&McG** | **N&al** |
|---|---|---|---|---|---|
| This study | 2001 | -1.3 (1.4) | -2.1 (2.3) | -1.7 (2.0) | -1.7(1.8) |
| | **2002** | **0.5 (0.9)** | **1.0 (1.4)** | **1.3 (1.3)** | **0.7 (1.1)** |
| | 2003 | 2.0 (0.7) | 3.3 (1.2) | 2.9 (0.9) | 2.6 (1.1) |
| | 2004 | 1.4 (1.3) | 2.4 (2.1) | 2.0 (1.9) | 1.9 (1.7) |
| Borges and Frankignoulle (2002) | 1996-1999 | 1.1 | 2.0 | 2.8 | 1.5 |
| **Emissions (Gmol C $yr^{-1}$)** | | | | | |
| This study | 2002 | 1.0 (3.7) | 1.9 (6.2) | 3.1 (5.4) | 1.3 (5.0) |
| Borges and Frankignoulle (2002)* | 1996-1999 | 2.3 | 4.2 | 4.4 | 3.1 |
| **% of the Scheldt estuary emission** | | | | | |
| Frankignoulle et al. (1998) | | 7 | 13 | 22 | 9 |
| Gazeau et al. (2005) | | 9 | 17 | 27 | 12 |

* $CO_2$ emission estimated from the annually integrated fluxes and a mean surface area of 2100 km².

The net annual emission from the Scheldt plume (Tab. 4) ranges between 1.0 (± 3.7) and 3.1 (± 5.4) Gmol C $yr^{-1}$, depending on the gas transfer velocity parameterization. This represents between 7 and 22% of the emission of $CO_2$ from the inner Scheldt estuary of 141 Gmol C $yr^{-1}$ given by Frankignoulle et al. (1998) and between 9 and 27% of the emission of $CO_2$ from the inner Scheldt estuary of 112 Gmol C $yr^{-1}$ given by Gazeau et al. (2005). These $CO_2$ emission estimates are below those given by Borges and Frankignoulle (2002) of 2.3 to 4.4 Gmol C $yr^{-1}$ because the latter values are derived from higher air-sea $CO_2$ flux estimates as discussed above, and to the use of a constant surface area for the plume of 2100 $km^2$ (here we used plume surface area values on cruise by cruise basis).

### 4.5.2. In the SBNS

Figure 28 shows for the seasonal variations of the spatial distribution of $pCO_2$ in the surface waters of the SBNS including estuarine plumes and adjacent areas (eastern English Channel), while Figure 29 show the monthly averages of $pCO_2$ and $\%O_2$ for the SBNS excluding the eastern English Channel.

For a given cruise, the $pCO_2$ distribution in the SBNS was quite homogeneous, as the amplitude of spatial variations ranged between 20 and 70 µatm (at most 50 µatm when estuarine plumes are excluded, *e.g.* for the area with salinities > 34), which was relatively small compared to the amplitude of the seasonal signal (~310 µatm, Fig. 29). Maximum and minimum $pCO_2$ values in the SBNS were observed in August and April (495 ± 51 and 184 ± 22 µatm, respectively). Higher $pCO_2$ values were observed along the BCZ (up to 900 µatm in August) related to the discharge of DIC rich waters from the heterotrophic inner Scheldt estuary. During winter, the SBNS was oversaturated in $CO_2$ with respect to the atmosphere, when temperature (~7.7 ± 0.2 °C in February) and biological activities ($O_2$ close to atmospheric equilibrium) were at the lowest. According to the spatial distribution of $\%O_2$ (data not shown) the onset of the diatom phytoplanktonic bloom (Rousseau et al. 2002) was in March, outside of the Scheldt and Rhine/Meuse plumes, due to better light penetration outside the plumes (Van Bennekom and Wetsteijn 1990). The phytoplanktonic bloom then spread within 3 weeks to the entire studied region as inferred by the strong $CO_2$ undersaturation in April ($pCO_2$ ~180 µatm) and high $\%O_2$ (120% for the SBNS, and up to 180% for the Scheldt plume, data not shown).
Figure 30 shows for the SBNS the annual cycle of mean surface $pCO_2$ and $pCO_2$@12.6°C based on data obtained from June 2003 to May 2004, with additional data from 2001 to 2002. Clear inter-annual variability was observed which can be explained by temperature, biological activities and mean salinity (*e.g.* estuaries discharges with higher DIC and nutrient content). Temperature effect on the $pCO_2$ dynamics from one year to another is shown by the comparison of $pCO_2$ and $pCO_2$@12.6°C during summer (e.g. mid-August 2002-2003; mid-September 2001-2002). In other cases inter-annual variability of $pCO_2$ was related to differences in biological activity.

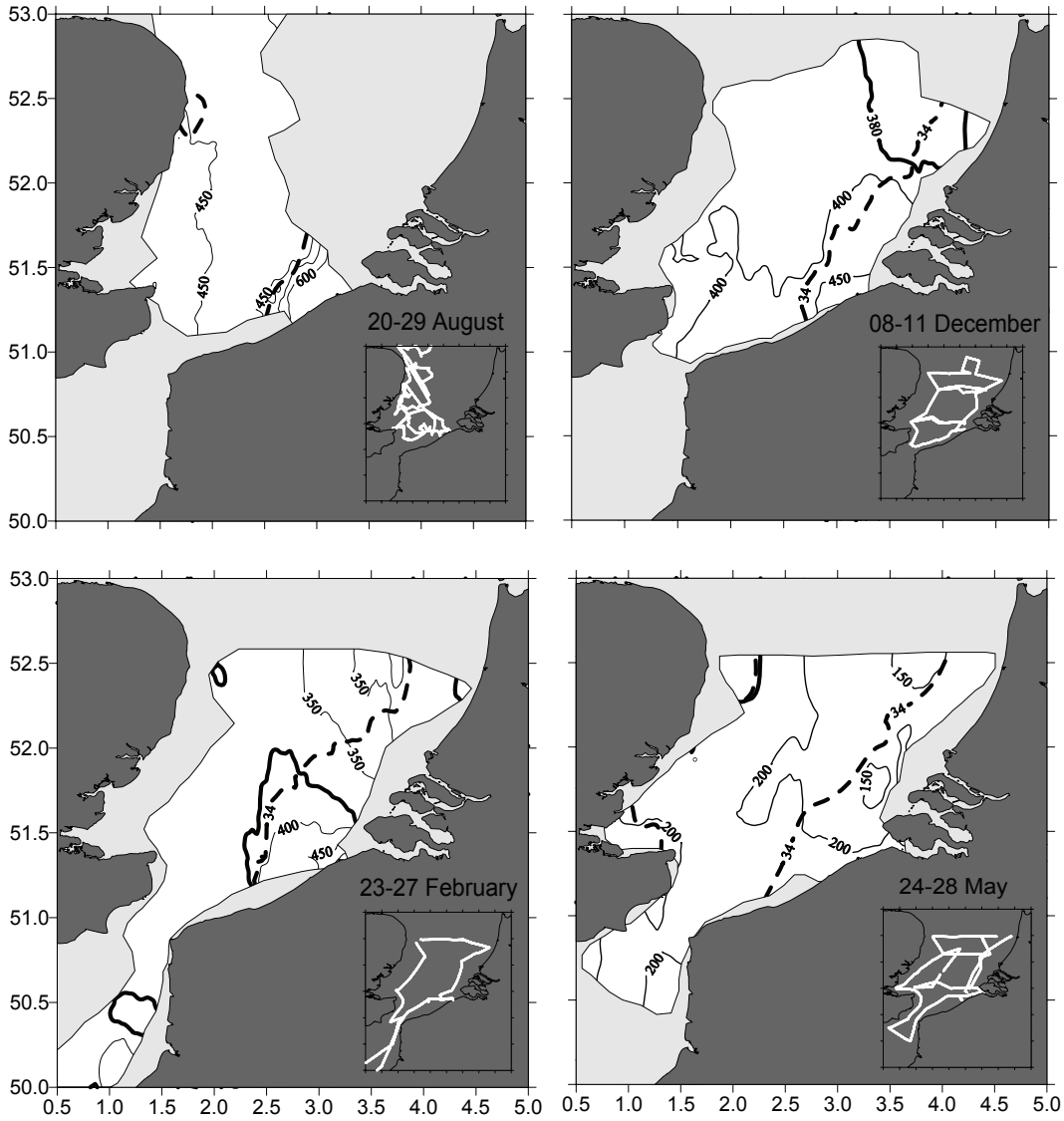


Figure 28. Surface distribution of $pCO_2$ in the SBNS and adjacent areas (English Channel) in August and December 2003, and in February and May 2004. The black line shows the limit of estuarine plumes defined by the 34 isohaline. The black bold line shows the atmospheric equilibrium. Inserts show the ship tracks. Adapted from Schiettecatte et al. (2007).

The largest differences occurred during the spring bloom when mean $pCO_2$ values in April 2001 and 2002 were, respectively, ~50 µatm lower and ~30 µatm higher than in 2004. Inter-annual differences among the mean $pCO_2$ are consistent with Sea-viewing Wide Field-of-view Sensor (SeaWiFS) level-3 chlorophyll-a data as discussed at length by Schiettecatte et al. (2006b).

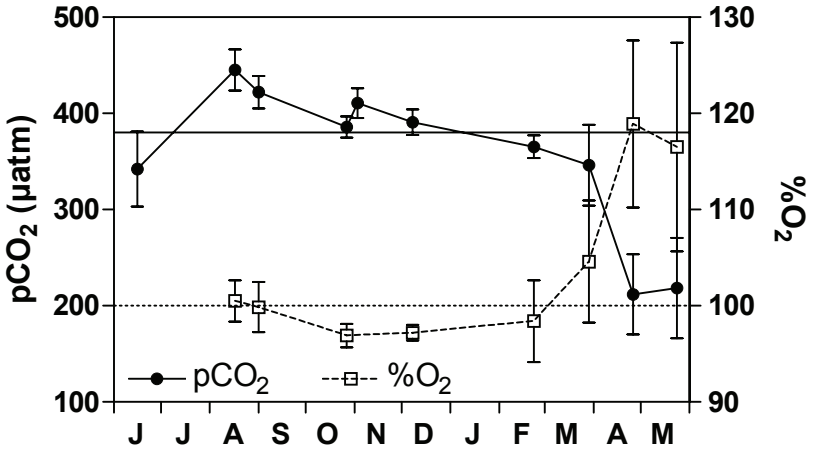


Figure 29. Monthly averaged values of $pCO_2$ (in µatm filled circles) and percentage of oxygen saturation ($\%O_2$, empty squares) for the SBNS (excluding estuarine plumes) from June 2003 to May 2004. Adapted from Schiettecatte et al. (2007).

Figure 30 shows that the late May 2002 cruise from the Thomas et al. (2004) study was carried out during the declining phase of the phytoplankton bloom, and that this data-set does not adequately account for the strong $CO_2$ under-saturation in the SBNS typically observed in mid-April during the peak of the phytoplankton bloom. This clearly highlights the need of high temporal resolution of measurements of $pCO_2$ to provide reliable annually integrated air-sea $CO_2$ fluxes, and to asses the different drivers of $pCO_2$, particularly in highly dynamic and heterogeneous coastal environments, such as estuarine plumes or proximal continental shelves.

From February to June, the SNBS was a sink of atmospheric $CO_2$ ranging from -0.1 to -18.7 mmol C $m^{-2}$ $d^{-1}$ (respectively, in June and April), in agreement with its trophic status (Fig. 31 and section 4.6.2). From August to December, the SNBS was a source of $CO_2$ to the atmosphere raging from 2.0 to 7.1 mmol C $m^{-2}$ $d^{-1}$, also in agreement with its trophic status. On an annual scale, the SBNS was a net sink for atmospheric $CO_2$ at a rate of -0.5 mol C $m^{-2}$ $yr^{-1}$. When estuarine plumes are excluded from the computations, annually integrated $F_{CO2}$ increased by about 30% (annual sink for atmospheric $CO_2$ at a rate of -0.7 mol C $m^{-2}$ $yr^{-1}$; data not shown).

Previous studies carried out in the SBNS which attempted to asses its role as a sink or source of $CO_2$ on an annual scale are presented in Table 5. Although the dataset from Frankignoulle and Borges (2001) did not cover a complete annual cycle, these authors hypothesized that the SBNS was an annual $CO_2$ sink. The $F_{CO2}$ values for April 1996 and May 1995 computed by Frankignoulle and Borges (2001) are about 2 times stronger than those computed in this study, due to differences in wind speed.

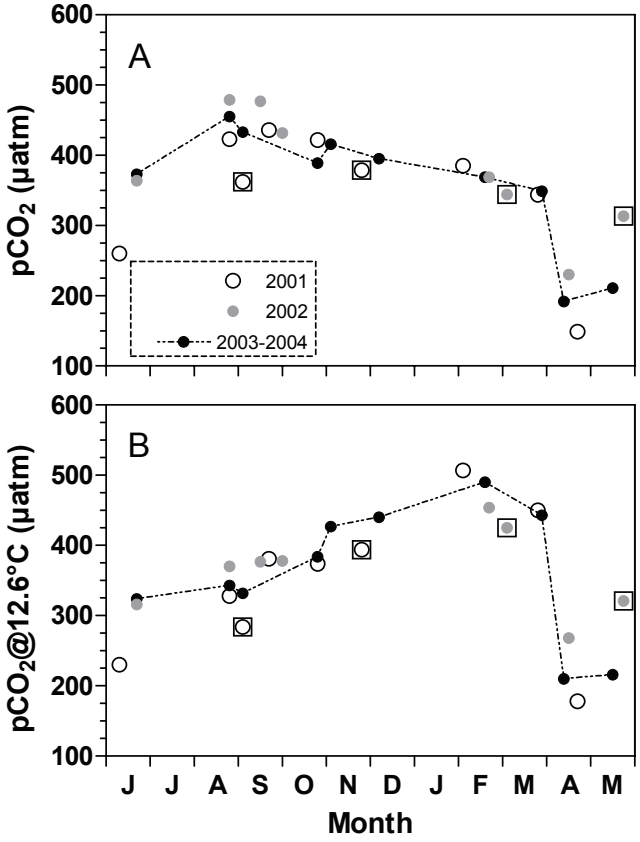


Figure 30 : Mean surface $pCO_2$ and $pCO_2$ normalized to a temperature of 12.6°C ($pCO_2$@12.6°C) in the SBNS (including estuarine plumes) gathered from 2001 to 2004. Annual cycle from June 2003 to May 2004 is shown as black circles, $pCO_2$ measured during 2001 and 2002 are represented respectively by empty and grey circles. Data from Thomas et al. (2004) are identified with a square. Adapted from Schiettecatte et al. (2007).

Frankignoulle and Borges (2001) used in their computations a mean $u_{10}$ of 9.6 m $s^{-1}$ in April 1996 against 6.2 m $s^{-1}$ in April 2004. In May 1995 and 2004, average $u_{10}$ were respectively 5.1 and 5.3 m $s^{-1}$ and $\Delta pCO_2$ values were similar. Frankignoulle and Borges (2001) computed $F_{CO2}$ with instantaneous $u_{10}$ (1 minute frequency) obtained during the 2 days transect, whereas $F_{CO2}$ in this study was computed with hourly $u_{10}$ data measured during the full duration of the cruise. The differences in $F_{CO2}$ are due to the strong non-linear relationship between *k* and $u_{10}$, which can lead to significant differences due to the wind speed frequency distribution and the averaging methods used (e.g. Bates and Merlivat 2001; Lüger et al. 2006). The high temporal resolution of the present study shows that the study by Thomas et al. (2004) did not capture the maximum extent of the $pCO_2$ minimum during spring in the SBNS. According to this study the SBNS (corresponding to the box 2 in their study) was an annual source of $CO_2$ at a rate of 0.2 mol C $m^{-2}$ $yr^{-1}$, while the present study identifies the SBNS as a $CO_2$ sink on an annual scale of -0.5 mol C $m^{-2}$ $yr^{-1}$.

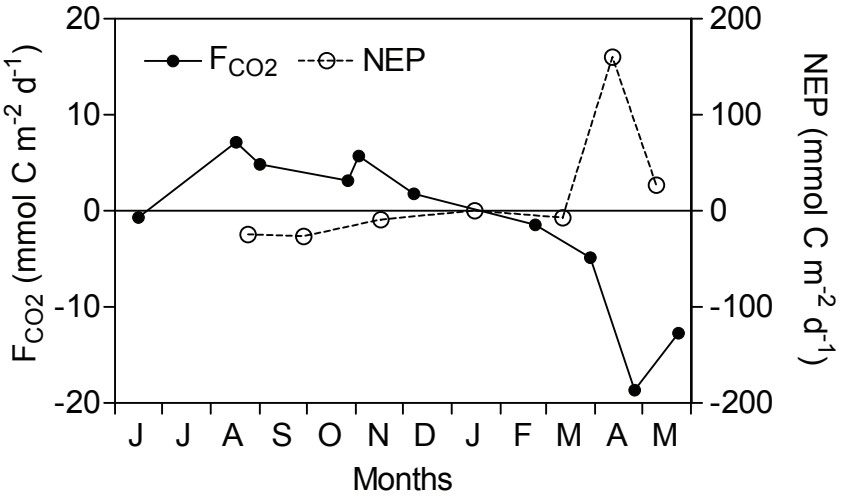


Fig. 31. Net ecosystem production (NEP in mmol C $m^{-2}$ $d^{-1}$, empty circles) based on a DIC mass balance computation and monthly air-sea $CO_2$ fluxes ($F_{CO2}$, mmol C $m^{-2}$ $d^{-1}$, filled circles) computed using the gas transfer velocity parameterization given by Nightingale et al. (2000) for the Southern Bight of the North Sea (SBNS). Adapted from Schiettecatte et al. (2007).

Table 5: Comparison of air-sea $CO_2$ fluxes ($F_{CO2}$ in mmol C $m^{-2}$ $d^{-1}$) in the Southern Bight of the North Sea (SBNS), from the present study and literature, computed using the gas transfer velocity parameterization from Wanninkhof (1992), and Wanninkhof and McGillis (1999), referred, respectively, as W and W&McG. Adapted from Schiettecatte et al. (2007).

| Month | this study | | | Frankignoulle and Borges (2001) | | Thomas et al. (2004) | |
|---|---|---|---|---|---|---|---|
| | $\Delta pCO_2$ | $F_{CO2\,[W]}$ | $F_{CO2[W\&McG]}$ | $\Delta pCO_2$ | $F_{CO2[W]}$ | $\Delta pCO_2$ | $F_{CO2[W\&McG]}$ |
| Sept. | 72 | 5.5 | 4.1 | | | 17.7 | 1.2 |
| Nov. | 37 | 7.4 | 7.5 | 5 | 2.5 | 16.5 | 2.4 |
| Apr. | -178 | -23.1 | -20.1 | -105 | -58.4 | | |
| May | -166 | -15.3 | -11.9 | -170 | -27.1 | -17.3 | -2.4 |

## 4.6. NET ECOSYSTEM PRODUCTION (NEP)

### 4.6.1. In the Scheldt Plume

4.6.1.1. NEP estimated by a stoichiometrically linked C/P mass balance budget (Land-Ocean Interaction in the Coastal Zone; LOICZ)

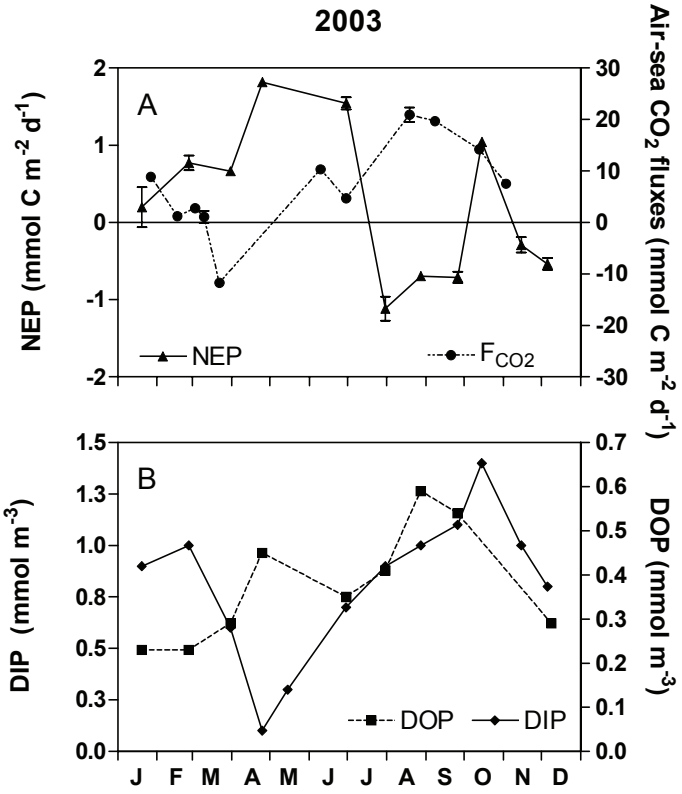


Figure 32. A: Left axis: monthly net ecosystem production (NEP; mmol C $m^{-2}$ $d^{-1}$; green triangles) in 2003 estimated from the Land Ocean Interaction in the Coastal Zone (LOICZ) budgeting procedure applied to dissolved inorganic phosphorus (DIP). Errors bars refer to standard errors computed from a Monte-Carlo procedure. Right axis: Averaged air-sea $CO_2$ fluxes ($F_{CO2}$ in mmol C $m^{-2}$ $d^{-1}$; blue circles) computed from $pCO_2$ data acquired in the whole plume (survey area approach), the gas transfer velocity parameterization as a function of wind speed given by Nightingale et al. (2000) and wind speed data from station Vlakte van de Raan. B: dissolved organic phosphorus (DOP) and DIP in mmol $m^{-3}$ in the Scheldt plume. Adapted from Schiettecatte et al. (2006).

A DIP budget in the Scheldt plume for year 2003 was carried out using the C/N/P stochiometrically LOICZ method given by Gordon et al. (1996). As the water column is well-mixed through the year, the Scheldt plume was considered as a one-layer box. Residual inputs and mixing fluxes from the inner Scheldt estuary as well as mixing fluxes with the SBNS were considered. DIP data in 2003 for the Scheldt plume and SBNS boxes were compiled from the CANOPY project. Additionally, data from van der Zee and Chou (2005), from the Belgian Marine Data Center (BMDC),

and from the EUROTROPH (Nutrients Cycling and the Trophic Status of Coastal Ecosystems; http://www.co2.ulg.ac.be /eurotroph/) were also included.

Figure 32 shows computed monthly NEP values in 2003 estimated for the Scheldt plume using the LOICZ modeling procedure applied to DIP (10 months sampling coverage in 2003), and air-sea $CO_2$ fluxes from the survey area of the Scheldt plume. From January to June and in October, the Scheldt plume was autotrophic (range 0.2 ± 3.0 to 1.8 ± 0.0 mmol C $m^{-2}$ $d^{-1}$) and heterotrophic the rest of the year (range -0.3 ± 0.1 to -1.1 ± 1.2 mmol C $m^{-2}$ $d^{-1}$). The strongest autotrophy was computed for April (1.8 ± 0.0 mmol C $m^{-2}$ $d^{-1}$) during the spring diatoms-*Phaeocystis* bloom when surface seawater were strongly undersaturated in $CO_2$ with respect to the atmosphere. Annually averaged NEP in the Scheldt plume was estimated to 0.2 ± 3.7 mmol C $m^{-2}$ $d^{-1}$, hence, a metabolic status not significantly different from balance.
The computed NEP values in spring during the phytoplanktonic bloom are too low to explain the decrease of $pCO_2$ during that period (Fig. 26, survey area approach). If we assume a mean TA of the Scheldt plume of 2450µmol $kg^{-1}$, a decrease of about 300µatm of the surface $pCO_2$ from early to mid March, and taking into account a mean air-sea $CO_2$ fluxes of about -5 mmolC $m^{-2}$ $d^{-1}$, the corresponding NEP is of about 6 mmolC $m^{-2}$ $d^{-1}$. This rough estimate is higher than the one based on DIP budget of 1 mmolC $m^{-2}$ $d^{-1}$ for the same period.
Several problems arise from the use of DIP in computing NEP in the Scheldt estuarine plume:
The first one deals with the ability of *Phaeocystis sp* to grow, under DIP depleted conditions, on dissolved organic phosphorus (DOP) by means of the alkaline phosphatase (AP). As the *Phaeocystis sp.* bloom occurs the after diatom bloom, the water column is depleted in DIP. In order to ensure their phosphate requirements, the *Phaeocystis* colonies de-repress (for DIP concentration below 0.5 mmol $m^{-3}$) the enzyme AP (Veldhuis and Admiraal, 1987; Van Boekel and Veldhuis, 1990). Chlorophyll-*a* (not shown) was highest during spring and consistent with the DIP decrease from February to end May due to photosynthetic activity whereas DOP increased during the same period (Figure 32). The first peak of DOP in April is associated to a release from phytoplanktonic cells whereas the second one in August is associated to bacterial activity (van der Zee and Chou 2005). NEP computed from the DIP mass balance during the spring bloom could be underestimated, because of the physiological adaptation of *Phaeocystis sp* to grow on DOP. However, DOP concentrations were still important throughout summer suggesting a continued remineralization by bacteria. Therefore, NEP computed from the DIP mass balance during summer could have lead to a significant underestimation of heterotrophy. As no DOP data were available for the inner Scheldt estuary and the SBNS boxes, it was not possible to integrate DOP in the present LOICZ budget.

The second caveats of the DIP budget comes from the use of the Redfield ratio in order to convert NEP values into carbon units. We assumed a molar C/P ratio of 106:1. However, *Phaeocystis sp* has two distinct forms during its life cycle. The first one is in the form of single flagellate cells that evolve to a colonial stage under low nutrients concentration. These colonies are characterized, by the presence of an extracellular matrix rich in polysaccharides, leading to a C/P molar ratio higher than 106:1 (Lancelot and Mathot 1987; Schoemann et al. 2005). In culture experiments, Jahnke (1989) showed that the C/P molar ratio of *Phaeocystis sp* under DIP deficient conditions ranged between 128:1 and 568:1. Using these two extreme values, the NEP computed for April 2003 would range between 2.2 and 9.7 mmol C $m^{-2}$ $d^{-1}$.
Finally, Gazeau et al. (2005) pointed out the fact that, due to abiotic processes such as DIP adsorption and desorption to and from suspended particles and/or sediment, the use of a C/P stoechiometrically linked budget to estimate NEP in the Scheldt inner estuary was strongly biased. These authors suggested the occurrence of a DIP net adsorption in the oligohaline part and DIP desorption in the marine part of the estuary due to changes in pH and ionic strength (see Froelich 1988). As suspended matter concentrations in the estuarine plume are of the same order of magnitude as in the mouth of the estuary, DIP desorption from suspended particles in the plume could be significant compared to DIP changes due to organic matter production and degradation. Gazeau et al. (2005) estimated potential DIP desorption rates in the marine part of the inner Scheldt estuary ranging between 0.2 and 0.8 mmol P $m^{-2}$ $d^{-1}$, which if applicable to our study site would have lead to a strong underestimation of NEP.

4.6.1.2. NEP in the Scheldt plume estimated by a DIC mass balance budget

The use of box model approaches to compute NEP requires the knowledge of water flows that are typically highly variable in coastal environments, and tend to introduce a large uncertainty that is difficult to estimate. A more simple approach relies on the temporal variation of DIC, whereby:

$$NEP = \frac{DIC_2 - DIC_1}{\Delta t}.d - \frac{F_{CO2(2)} + F_{CO2(1)}}{2} \qquad (6)$$

where $DIC_1$ and $DIC_2$ are DIC values from 2 consecutive cruises, $F_{CO2(1)}$ and $F_{CO2(2)}$ are the air-sea $CO_2$ fluxes from 2 consecutive cruises, Δt is the time interval between 2 consecutive cruises and d is the depth of the mixed layer.
Such an approach is suited for permanently well-mixed systems such as the SBNS and the Scheldt plume, as knowledge of the mixed layer depth is not required. This method relies on the assumption that the production and degradation of organic

matter, and air-sea $CO_2$ exchange are the main drivers of $CO_2$ dynamics (and that other processes such as $CaCO_3$ production/dissolution are negligible). Such an assumption holds true in the SBNS and the Scheldt plume based on current understanding of $CO_2$ dynamics in these regions (Borges and Frankignoulle 1999; 2002; Frankignoulle and Borges 2001; Gypens et al. 2004; Schiettecatte et al. 2006; 2007). The major caveat of the method is the assumption that the advective inputs/outputs of $CO_2$ are constant between two steps of the computation. This source of uncertainty can be assumed minimal in the present case because for time steps of the computations lower than the water residence time, and invariance of $CO_2$ advective inputs/outputs can be assumed. In the Scheldt plume the average time step of the computations was 21 d for an average water residence time of 60 d in the Belgian Coastal Zone (BCZ) (Lancelot et al. 2005).
TA was computed from :

$$TA = 3928.6 - 46.156.S \quad (r^2 = 0.872, p<0.0001) \qquad (7)$$

where S is salinity, established from 742 measurements from 26 cruises carried out from 1996 to 2001 (Borges and Frankignoulle 1999; Borges unpublished; Schiettecatte unpublished). DIC was computed from measured $pCO_2$ and TA computed from salinity. $F_{CO2}$ was computed using equation (1).
Figure 33 shows NEP computed from $pCO_2$ at the reference station in front of the Zeebrugge harbour, that is assumed representative of $CO_2$ dynamics of the Scheldt estuarine plume (Borges and Frankignoulle 1999; 2002). A transient and strongly autotrophic period occurs in spring that peaks in slightly different months from year to year (early April in 2001 and 2002, mid April in 2003 and 2004), and that is different in amplitude with maximal values ranging from 269 mmol $m^{-2}$ $d^{-1}$ in 2004 to 134 mmol $m^{-2}$ $d^{-1}$ in 2003. This strongly autotrophic period can be ascribed to the *Phaeocystis* bloom in agreement with the trends previously described for the BCZ (e.g. Gypens et al. 2004; Lancelot et al. 2005; 2007; Breton et al. 2006). A marked diatom bloom preceding the *Phaeocystis* bloom is only apparent from our NEP estimates in 2003. The *Phaeocystis* bloom is followed by a marked heterotrophic period after which an increase in NEP is observed. This increase in NEP leads to a net autotrophic event in 2001 and 2003, and to a balanced metabolic status in 2002 and 2004. This increase in NEP can be ascribed to the summer diatom bloom that is known to be very variable in timing and amplitude in the BCZ (Breton et al. 2006; Lancelot et al. 2007). Late summer is characterized by net heterotrophy that decreases during fall, and a nearly balanced metabolic status is observed in winter.

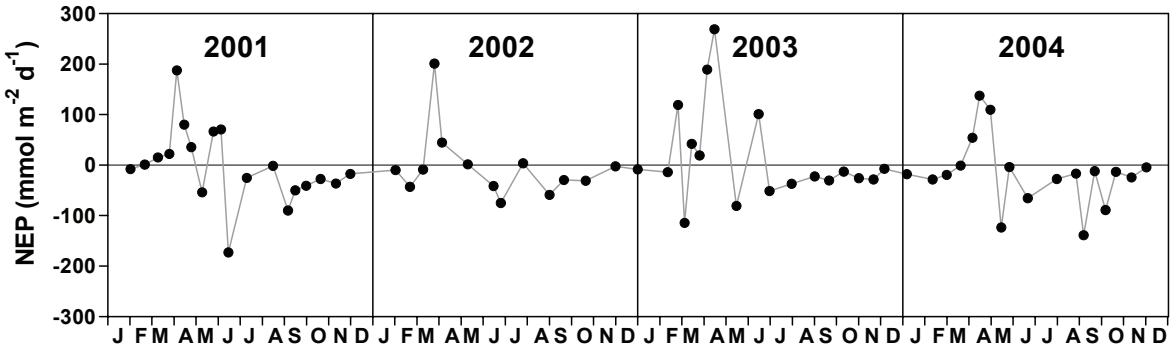


Figure 33. Time series of net ecosystem production computed from a 0-D mass balance of dissolved inorganic carbon computed from $pCO_2$, in the Scheldt plume at a fixed station off the Zeebrugge harbor. Borges et al. (2007).

At annual scale the Scheldt river plume acted as a net heterotrophic system in 2001, 2002 and 2004, but acted as a net autotrophic system in 2003 (Tab. 6). Net heterotrophy of the Scheldt river plume has been previously shown by Borges and Frankignoulle (2002) based on a simple organic matter input/output budget, to explain the annual emission of $CO_2$ to the atmosphere that is only partly due to the input of $CO_2$ from the Scheldt inner estuary. The net heterotrophy of the Scheldt river plume must be subsidised by external inputs of organic carbon that can originate from the Belgian coast and/or from the Scheldt inner estuary. The input of organic matter from the Scheldt inner estuary estimated by Soetaert and Herman (1995) corresponds to a potential organic matter degradation ranging between 0.3 and 0.6 mol $m^{-2}$ $yr^{-1}$ for, respectively, a Scheldt plume surface area ranging between 2000 and 800 $km^2$ (Borges and Frankignoulle 2002). Wollast (1976) provides a higher estimate of the input of organic matter from the Scheldt inner estuary that can sustain a potential organic matter degradation ranging between 0.8 and 2.0 mol $m^{-2}$ $yr^{-1}$. Finally, Wollast (1983) estimated the input of organic carbon from the Belgian coast that can sustain a potential organic matter degradation ranging between 0.7 and 1.8 mol $m^{-2}$ $yr^{-1}$. These inputs of organic matter are of the order of magnitude of the NEP values we computed.

The much stronger springtime NEP and annual net autotrophy observed in 2003 compared to the other years could be due to a combination of two processes. Wintertime freshwater discharge was stronger in 2003 than in the other years (Tab. 6). We used the average value of freshwater discharge in January and in December of the previous year, since the freshwater residence time in the Scheldt inner estuary ranges between 30 and 90 d. Hence, the freshwater water discharges during these months are those that can be assumed relevant for the productive season (from February to April) in terms of nutrient inputs from the Scheldt inner estuary. We hypothesize that in 2003 there was a stronger input of nutrients compared to the other years, while the input of organic matter was similar to other years. In the

Scheldt inner estuary, the input of nutrients from diffuse sources are dependent on freshwater discharge, while organic matter comes mainly from point sources independently of freshwater discharge. This would lead to a stronger gross primary production (GPP) in 2003 from the additional nutrient inputs, but allochtonous organic carbon inputs would sustain a similar level of heterotrophy than in the other years. Gypens et al. (2004) showed by comparing two contrasted years that annual GPP in the BCZ could increase by about 27% for an increase of wintertime fresh water discharge of about 250 $m^3$ $s^{-1}$. Also, incoming PAR was more favourable in 2003 during the productive months (February, March and April, data not shown), and could explain the marked autotrophy associated to the diatom bloom in mid-February. Despite the fact that the Scheldt river plume was net autotrophic in 2003, it still acted as net source of $CO_2$ to the atmosphere (Tab. 6). This confirms that a fraction of this $CO_2$ emission is sustained by the inputs of $CO_2$ from the Scheldt inner estuary (Borges and Frankignoulle 2002; Schiettecatte et al. 2006a) that would also be expected to increase with freshwater discharge.

Table 6. Average Scheldt fresh water discharge (Q) from January and December of the previous year, and annual averages of $pCO_2$, air-sea gradient of $pCO_2$ ($\Delta pCO_2$), $F_{CO2}$ and NEP at a fixed station in the Scheldt plume off the Zeebrugge harbor. Borges et al. (2007).

| | Q ($m^3$ $s^{-1}$) | $pCO_2$ (µatm) | $\Delta pCO_2$ (µatm) | $F_{CO2}$ (mol $m^{-2}$ $yr^{-1}$) | NEP (mol $m^{-2}$ $yr^{-1}$) |
|---|---|---|---|---|---|
| 2001 | 348 | 481 | 107 | 3.6 | -4.2 |
| 2002 | 302 | 480 | 97 | 3.2 | -3.8 |
| 2003 | 393 | 527 | 136 | 4.6 | 2.4 |
| 2004 | 210 | 533 | 153 | 6.6 | -5.7 |

The stronger annual heterotrophy in 2004 than in 2001 and 2002 could be due to a transient accumulation of part of the excess organic matter produced in 2003. The water residence time in the BCZ is highly variable but can be as long as 216 d (Lancelot et al. 2007) and is assumed to be on average 60 d (Lancelot et al. 2005). Hence, we hypothesize that part of the non-steady accumulation of organic matter from 2003 to 2004 occurred in the sediments. Sedimentation of organic matter is important in the BCZ, representing about 20% of annual GPP (Lancelot et al. 2005), in agreement with the fact that the sediments in the BCZ are exceptionally rich in organic carbon compared to the rest of the North Sea (Wollast 1976; de Haas et al. 2002).

### 4.6.2. In the SBNS

We use the same approach to compute NEP as in section 4.6.1.2., based on the temporal DIC variations according to the equation (6), from August 2003 to May 2004 (Fig. 31). The SBNS was heterotrophic from mid-August to March (-6.6 to -24.2 mmol

C $m^{-2}$ $d^{-1}$), and was autotrophic from April to May, with strongest NEP value in April (160 mmol C $m^{-2}$ $day^{-1}$). At an annual scale the SBNS was strongly autotrophic at a rate of ~16.9 mmol C $m^{-2}$ $d^{-1}$. When estuarine plumes were excluded from the computations (data not shown), annually integrated NEP remained relatively unchanged (16.7 mmol C $m^{-2}$ $day^{-1}$). However, the SBNS (excluding the estuarine plumes) was autotrophic from mid-February to May (14.2 to 139.3 mmol C $m^{-2}$ $day^{-1}$), with strongest values in April (139.3 mmol C $m^{-2}$ $day^{-1}$). Heterotrophy was stronger from August to mid-January (-13.2 *versus* -21.0 mmol C $m^{-2}$ $d^{-1}$, mean NEP values for that period when excluding and including estuarine plumes, respectively). Estuarine plumes receive nutrient inputs that can support higher GPP, but during summer heterotrophy is also stronger due to the higher organic matter availability from the spring phytoplankton blooms, and to a lesser extent due to the inputs of organic matter from inner estuaries. These trends in NEP are in agreement with previous studies in the BCZ and the Scheldt estuarine plume (Gypens et al. 2004; Schiettecatte et al. 2006a).

These NEP values at annual scale and for the productive period (from February to August, 39.2 mmol C $m^{-2}$ $day^{-1}$, including estuarine plumes) are slightly higher but in fair agreement with those reported in the SBNS by Bozec et al. (2006), respectively, 10.1 and 33.3 mmol C $m^{-2}$ $day^{-1}$. These authors estimated NEP from the data-set of Thomas et al. (2004), with a DIC mass balance at the scale of the whole North Sea, based on the water flows from European Regional Seas Ecosystem Model (Lenhart and Pohlmann 1997) and using International Council for the Exploration of the Sea (ICES) boxes (the SBNS is divided into 2 ICES boxes). As mentioned above, the peak of phytoplanktonic bloom was not fully captured by the underlying data-set, which can explain the slightly higher NEP values from our study, although the differences could also be due the methodological approaches or inter-annual variability. Our annual integrated NEP value is also in good agreement with the NEP value of 15.3 mmol C $m^{-2}$ $d^{-1}$ computed for the SBNS by Gattuso et al. (1998) based on the GPP and community respiration measurements of Joiris et al. (1982).

## 4.7. DIN AND DIP BUDGETS IN THE SBNS

Inorganic N and P nutrient budgets were computed using the LOICZ methodology (Gordon et al, 1996). The SBNS was divided in 3 boxes: the Scheldt River plume corresponding more or less to the BCZ, the Rhine River Plume and the central SBNS. Budgets were calculated for 6 consecutive seasonal situations between September 2003 and May 2004 using data collected within the CANOPY project, from the NIOO-CEME monitoring program for the Scheldt mouth and from the Dutch WATERBASE database for the Rhine mouth. Additionally, information about the volumes of water entering the SBNS through the Strait of Dover were from Laane et al. (1996) who calculated monthly average water fluxes over a 20 year interval using the NORWECOM model.

### 4.7.1. River Plumes

Results are presented in figure 34. Both the Scheldt and Rhine river plumes are sinks for DIP and DIN whatever the period considered. The Scheldt Plume retains between 60 and 70 % of entering DIP and 70 to 75 % of entering DIN from September to February. In March and May, the retention increase to more than 80% of DIP and DIN. The Rhine plume retains between 30 and 90 % of DIP and 40 to 80% of DIN and showed stronger seasonal variations. Highest retention occurs during the spring and summer months (September, March and May).

Net retention of DIP in the river plumes can be due to net uptake by organisms but also to abiotic processes like adsorption of $PO_4$ onto particulate material. In both cases, DIP ends up in the particulate phase and can be exported to adjacent areas (central SBNS) or buried in the sediments. As biotic processes are influenced by seasonal variables (temperature, light, …) and abiotic processes not, our results may suggest a more important contribution of abiotic processes in the Scheldt Plume than in the Rhine Plume.

Net retention of DIN in the river plumes can be due to net DIN uptake by organisms and to denitrification. While the first process leads to the synthesis of organic N which can be further exported to adjacent areas as the open sea, denitrification represents a loss of N from the system.

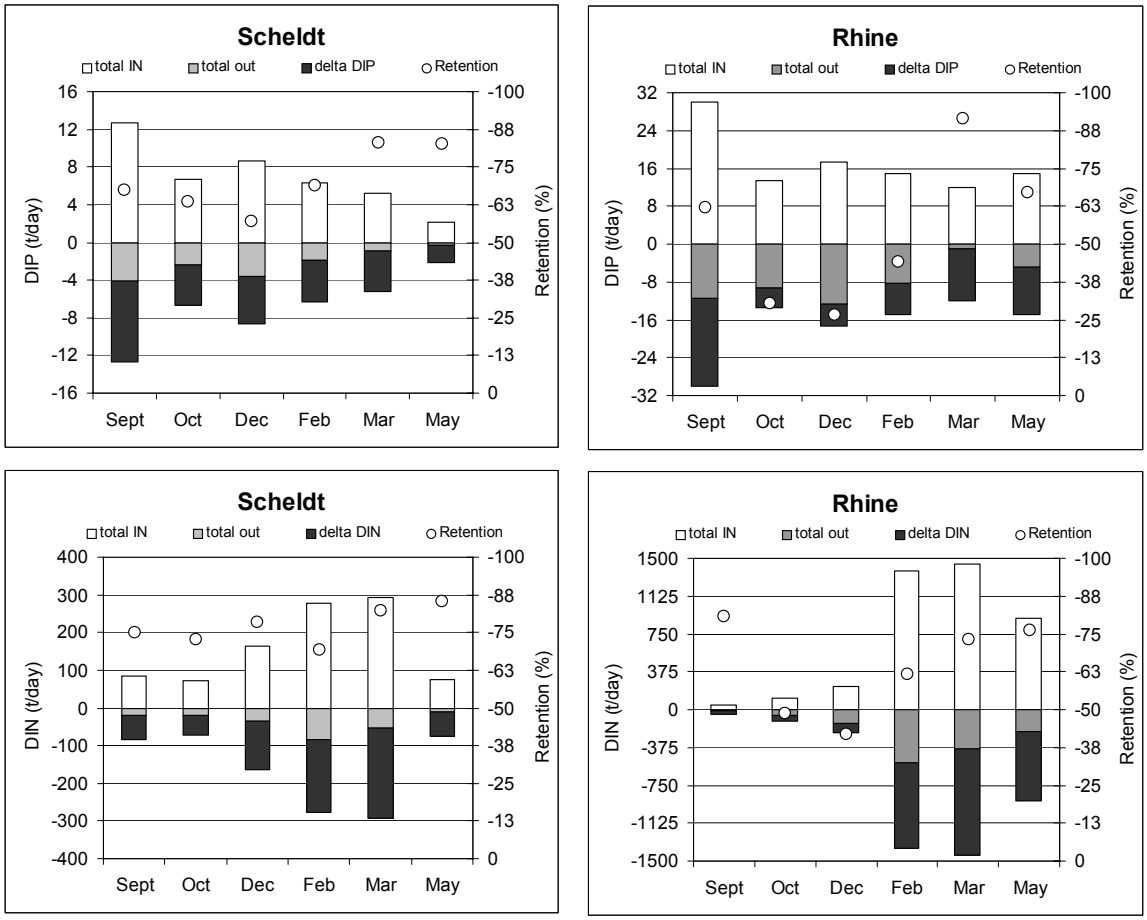


Figure 34. Input (total IN) and output (total out) fluxes of DIP and DIN in the river plumes of the Scheldt and Rhine Rivers. Net production of DIP and DIN (delta DIP, delta DIN) and relative retention of DIP and DIN (%). Positive values show sources, negative values show sinks.

### 4.7.2. Central SBNS

DIP and DIN can enter the SBNS through the river plumes and through incoming North Atlantic waters flowing from the Channel. Although concentrations in English channel waters are much lower than in river plume waters, the huge volumes of seawater from the English channel represent the most important DIP and DIN input in the region (Fig. 35). Unfortunately it is also a flux submitted to very large variability (Brion et al., 2004). Therefore numbers should be interpreted with great care.

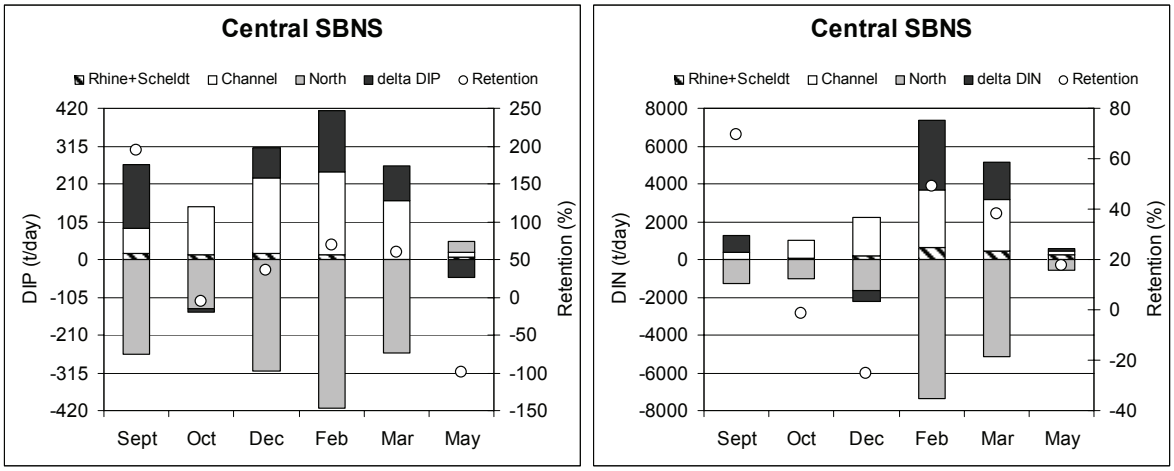


Figure 35. Input and output fluxes of DIP and DIN in the central SBNS. Net production of DIP (delta DIP) and DIN (delta DIN) and relative retention of DIP and DIN (%).
Positive values show sources, negative values show sinks.

The central part of the SBNS is most of the time a source for DIP from September to March. This may be the result of DIP regenerated from imported organic matter. Sources may be plumes (we have seen that the plumes were net sinks for DIP and could export P as organic compounds) and English channel waters. Only in May, a period of high phytoplankton biomass, the region acted as a net DIP sink consuming all the P entering from the Channel but also importing DIP from the Northern boundary (Central North Sea).
The Central part of the SBNS could either represent a net sink for DIN (with 2 to 25 % inputs being retained in October and December 2003) or a source. This source represents between 18 and 80 % of all DIN inputs in the system and shows the dominance of DIN regenerating processes in this central part, even during phytoplankton blooms.

As pointed out before, large uncertainties are linked to the estimation of nutrient inputs by the English channel. We tried to estimate this variability by changing the Channel water flux and calculating how this affected the estimated DIN and DIP budgets. Increasing or decreasing the Channel water flux by as much as a factor 2 did not result in major changes in the estimated delta DIN and delta DIP (figure 36) and supports our previous conclusions.

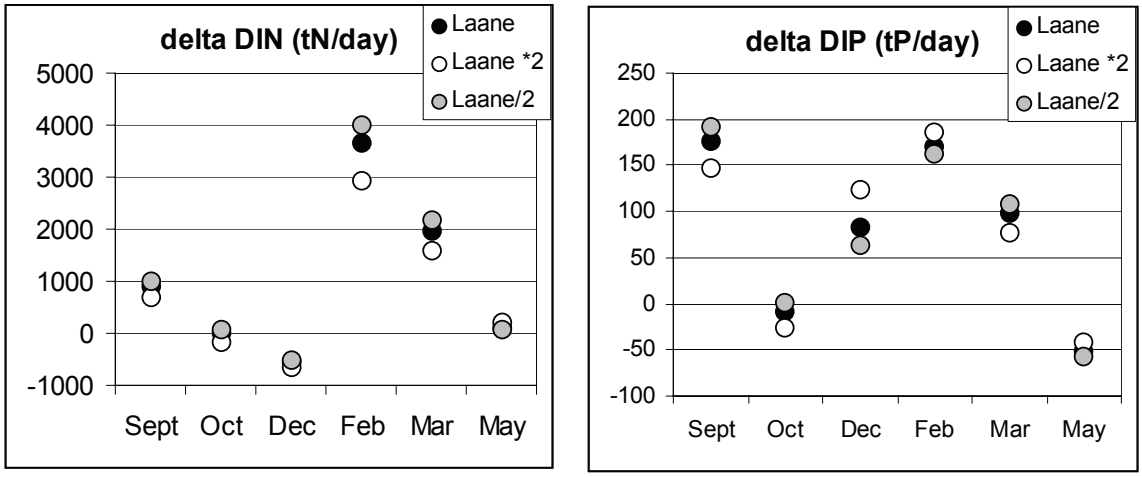


Figure 36. Effect of changing the Channel water flux on the net DIN and DIP production of the SBNS. Laane: as reported in Laane et al 1996, Laane*2: 2 times the Laane values, Laane /2: Laane values divided by 2. Positive values show sources, negative values show sinks.

# 5. GENERAL DISCUSSION

## 5.1. COUPLING BETWEEN N, C AND P DYNAMICS IN THE SBNS

### 5.1.1. Pelagic DIN uptake and primary production in the SBNS.

We calculated the average of the measured DIN uptake and primary production for the whole SBSN to evaluate the coupling between de C-fixation and DIN assimilation by phytoplankton. There is a remarkable clear correlation (Fig. 37) between de DIN utilization and primary production, with a C/N ratio of 6.5 very close to the Redfield-ratio of 6.6.

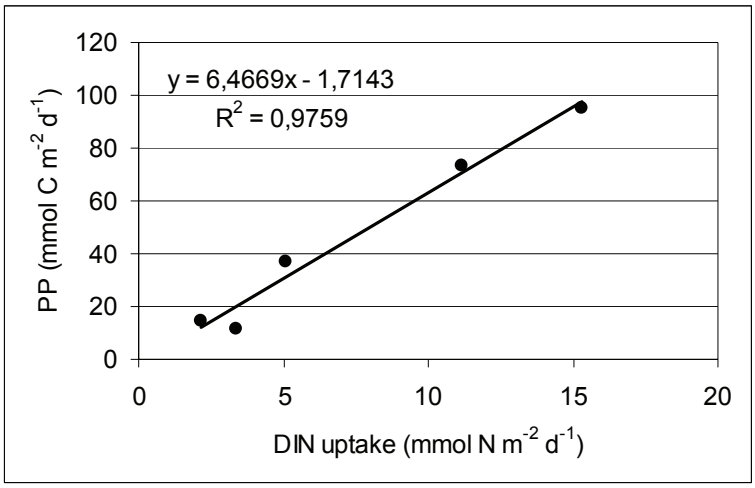


Figure 37. Average primary production (PP) and DIN uptake in the SBNS as extrapolated from the measurements (see 4.4.1 and 4.4.2).

### 5.1.2. Whole Net Ecosystem DIN-DIC-DIP Dynamics.

Whole Net Ecosystem DIN, DIP and DIC productions were estimated using various approaches within this project (see 4.6 and 4.7) and correlations between N and C, and P and C are presented in figures 38. The interpretation of the results should be made with great care, because of the different methodologies used for the DIC compared to the DIN and DIP, however some interesting features can be described. Two contrasting situations are observed for the fall-winter and spring seasons.

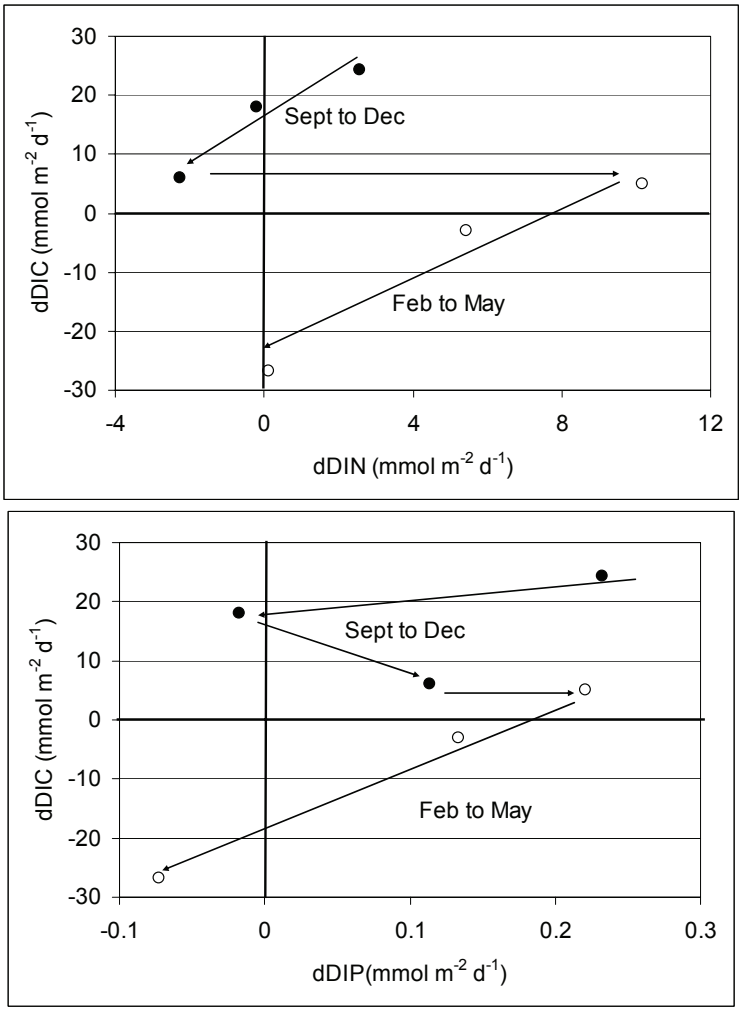


Figure 38. Correlations between NEP of DIC (dDIC) and DIP (dDIP) (top), and between NEP of DIC and DIN (dDIN) in the SBNS.

The C-N correlations (Fig. 38) show for both seasons similar slopes with a C:N ratio around 3.5. This is lower than the Redfield ratio but still characteristic of biological material. This suggests that whatever the season there is a DIC production sustained by OM with a high C:N ratio, either of terrestrial (estuarine) origin or from the sediment. This is in agreement with the fact that consumption of DIC by primary production exceeds the net ecosystem DIC production (section 5.2). The other possible cause is a large removal of DIN by denitrification in agreement with the fact that net pelagic DIN production largely exceeds net ecosystem DIN production (section 5.2). There was no C-P correlation in fall-winter but in spring, the slope of the correlation showed a C:P ratio of 109, very close to the Redfield ratio. However, for both the C-N and C-P correlations, the intercepts are different from 0 showing that primary production and respiration are not the only players in the DIC-DIN-DIP dynamics with the presence of unrelated DIC, DIN and DIP sources our sinks.

## 5.2. PELAGIC VS WHOLE ECOSYSTEM C AND N DYNAMICS.

Measured pelagic DIN uptake and regeneration rates (section 4.4.2) can be extrapolated to the whole SBNS (Scheldt plume and open sea area) and compared to net ecosystem DIN production (section 4.7). In the same way, measured primary production (section 4.4.1) can be compared to net ecosystem DIC productions (section 4.6).

Table 7. Pelagic and ecosystem production of DIN (dDIN) and DIC (dDIC) in the SBNS.

| | Pelagic dDIN mmol $m^{-2}$ $d^{-1}$ | Ecosystem dDIN mmol $m^{-2}$ $d^{-1}$ | Pelagic dDIC phyto mmol $m^{-2}$ $d^{-1}$ | Ecosystem dDIC mmol $m^{-2}$ $d^{-1}$ |
|---|---|---|---|---|
| 01/09/03 | -3.89 | 2.56 | -74.81 | 24.39 |
| 27/10/03 | 98.82 | -0.20 | -10.76 | 18 |
| 23/02/04 | 75.34 | 10.16 | -14.78 | 5 |
| 29/03/04 | 127.58 | 5.45 | -36.90 | -3 |
| 24/05/04 | 33.51 | 0.11 | -98.73 | -26.71 |

For nitrogen (Table 7), we can see that except for September, net pelagic DIN production largely exceeds net ecosystem DIN production. There is a net production of DIN in the water column but this DIN does not accumulate. An important additional DIN sink is thus needed to maintain this situation in balance. The only process that could explain this sink is denitrification in the sediments which should then occur at rates between 33 to 122 mmol N $m^2$ $d^{-1}$. Although there are only very few denitrification measurements in the SBNS, these rates are huge compared to the existing literature estimates (from 0.002 to 0.7 mmol N $m^{-2}$ $d^{-1}$, Brion et al. 2004). Possibly our extrapolation of in-situ measured transformation rates for a few stations (5) to the entire area is inappropriate.

For DIC, the consumption of DIC by primary production exceeds the net ecosystem DIC production showing the importance of heterotrophic respiration processes. These heterotrophic respiration processes account for a DIC production between 20 (in February) and 99 mmol $m^{-2}$ $d^{-1}$ (Sept) and was highest during the periods of highest phytoplanktonic activity and biomass (Sept and May).

# 6. CONCLUSIONS

The CANOPY project aimed to determine the importance of the internal cycling processes of uptake and regeneration of carbon, nitrogen and phosphorus in the SBNS, a marine area receiving large riverine inputs from the Scheldt and Rhine rivers, but also under the large influence of inflowing English channel waters through the Strait of Dover.

The SBNS area was characterized by the presence of 2 large river plumes with high levels of nutrients extending in the Belgian and Dutch costal waters, a central part of the SBNS with lower nutrient levels. DIN and DIP levels in these regions varied seasonally and were lowest during the periods of highest phytoplankton biomass, in spring and late summer. Additionally, organic N and P represented important fractions of the total N and P. In the central waters, DON, DOP and POP dominated the N and P pools in summer, but their relative importance was more limited in the river plumes.

For the pelagic system, DIC, DIN and DIP uptake measurements varied seasonally and were highest during the spring phytoplankton bloom, and for some stations, at the end of the summer phytoplankton bloom. Additionally, the uptake of DIN and primary production were well correlated with a C:N ratio of 6.5 very close to Redfield ratio of 6.6. The regeneration of DIN was in general largely exceeding the uptake except in spring, where we have a more balanced situation. The regeneration of DIP also represented a large fraction of the DIP taken up. Heterotrophic processes are thus very active in the SBNS. They clearly dominate the pelagic N cycling, and are in balance with uptake processes for DIP.

At ecosystem scale, it was demonstrated that the Scheldt plume was net heterotrophic and acted as an important source of $CO_2$ for the atmosphere. In contrast, the Scheldt plume also acted as an active sink for both DIN and DIP probably due to active denitrification and physical adsorption processes in this organic matter and SPM rich environment. In contrast, the open water of the SBSN was autotrophic and acted as a sink for $CO_2$. Again in contrast, there was a net production of DIN and DIP. The detailed comparison of DIN and DIP budgets with DIC budgets showed that correlations exist but were not straightforward. In general, correlations showed a C:N ratio of 3.5 (the whole year) and a C:P ratio of 109 (only in spring) very close to the characteristic ratio of phytoplankton biomass synthesis and degradation. This suggests that whatever the season there is a DIC production sustained by OM with a high C:N ratio, either of terrestrial (estuarine) origin or from the sediment. This is agreement with the fact that consumption of DIC by primary production exceeds the net ecosystem DIC production. The other possible cause is a large removal of DIN by denitrification in agreement with the fact that net pelagic DIN production largely exceeds net ecosystem DIN production. However, the correlation

lines did not pass through 0 showing that primary production and respiration are not the only players in the DIC-DIN-DIP dynamics with the presence of unrelated DIC, DIN and DIP sources our sinks.

# 7. AKNOWLEDGEMMENTS

We thank the captains and crew of the *R.V. Belgica,* for full support during the CANOPY cruises, Joan Backers (Management Unit of the North Sea Mathematical Models, MUMM) and the crew of the *R.V. Belgica* for their help in running the unattended underway $pCO_2$ system, MUMM for thermosalinograph data. AVB is a research associate at the Fonds National de la Recherche Scientifique.

# 8. REFERENCES

Ammerman JW and Azam F (1985) Bacterial 5'-nucleotidase activity in aquatic ecosystems: A novel mechanism of phosphorus regeneration. Science 227:1338-1340.

Ammerman JW and Azam F (1991a) Bacterial 5'-nucleotidase activity in estuarine and coastal marine waters: characterization of enzyme activity. Limnol. Oceanogr. 36:1427-1436.

Ammerman JW and Azam F (1991b) Bacterial 5'-nucleotidase activity in estuarine and coastal marine waters: Role in phosphorus regeneration. Limnol. Oceanogr. 36:1437-1447.

Ammerman JW (1993) Microbial cycling of inorganic and organic phosphorus in the water column. 649-660. In: Handbook of methods in aquatic microbial ecology. Eds. Kemp PF, Sherr BF, Sherr EB and Cole JJ. Lewis Publishers, New York, USA.

Bates NR and Merlivat L (2001) The influence of short-term wind variability on air-sea $CO_2$ exchange. Geophysical Research Letters 28:3281-3284.

Benson BB and Krause D (1984) The concentration and isotopic fractionation of oxygen dissolved in freshwater and seawater in equilibrium with the atmosphere. Limnology and Oceanography 29:620-632.

Björkman K and Karl DM (1994) Bioavailability of inorganic and organic phosphorus compounds to natural assemblages of microorganisms in Hawaiian coastal waters. Mar. Ecol. Prog. Ser. 111:2665-273.

Borges AV, Delille B and Frankignoulle M (2005) Budgeting sinks and sources of CO2 in the coastal ocean: Diversity of ecosystems counts. Geophys. Res. Let. 32 (14).

Borges A.V., L.-S. Schiettecatte, G. Abril, B. Delille & F. Gazeau (2006) Carbon dioxide in European coastal waters, Estuarine, Coastal and Shelf Science, 70(3), 375-387

Borges A.V., K. Ruddick, B. Delille & L.-S. Schiettecatte (2007) Net ecosystem production and carbon dioxide fluxes in the Scheldt estuarine plume, submitted

Borges AV (2005) Do we have enough pieces of the jigsaw to integrate $CO_2$ fluxes in the coastal ocean? Estuaries 28 (1):3-27.

Borges AV and Frankignoulle M (1999) Daily and seasonal variations of the partial pressure of $CO_2$ in surface seawater along Belgian and southern Dutch coastal areas. Journal of Marine Systems 19:251-266.

Borges AV and Frankignoulle M (2002) Distribution and air-water exchange of carbon dioxide in the Scheldt plume off the Belgian coast. Biogeochemistry 59: 41-67.

Bouwman AF, Van Drecht G, Knoop JM, Beusen AHW and Meinardi CR (2005) Exploring changes in river nitrogen export to the world's oceans. Global Biogeochem. Cycles 19, GB1002, doi: 10.1029/2004GB002314.

Bozec Y, Thomas H, Schiettecatte L-S, Borges AV, Elkalay K and de Baar HJW (2006) Assessment of the processes controlling the seasonal variations of dissolved inorganic carbon in the North Sea. Limnology and Oceanography 51(6):2746-2762.

Breton E, Rousseau V, Parent J-Y, Ozer J and Lancelot C (2006) Hydroclimatic modulation of diatom/Phaeocystis blooms in nutrient-enriched Belgian coastal waters (North Sea). Limnology and Oceanography 51(3):1401–1409.

Brion N, Baeyens W, De Galan S, Elskens M and Laane RWPM (2004) The North Sea: source or sink for nitrogen and phosphorus to the Atlantic Ocean. Biogeochemistry 68:277-296.

Christian JR, Karl DM (1995) Measuring bacterial ectoenzyme activities in marine waters using mercuric chloride as a preservative and a control. Mar Ecol Prog Ser 123:217-224.

Copin-Montégut C (1988) A new formula for the effect of temperature on the partial pressure of carbon dioxide in seawater. Marine Chemistry 25:29-37.

Copin-Montégut C (1989) A new formula for the effect of temperature on the partial pressure of carbon dioxide in seawater. Corrigendum. Marine Chemistry: 27:143-144.

Dafner E, De Galand S, and Goeyens L (1999) Microwave digestion of organic substances, a useful tool for dissolved organic nitrogen measurements. Water Research 33:548-554.

de Haas H, van Weering TCE and de Stigter H (2002) Organic carbon in shelf seas: sinks or sources, processes and products. Continental Shelf Research 22: 691-717.

Diaconu C, Brion N, Elskens M and Baeyens W (2005) Validation of a dynamic ammonium extraction technique for the determination of $^{15}N$ at enriched abundances. Analytica Chimica Acta 554:113–122.

Dickson AG (1990) Thermodynamics of the dissociation of boric acid in synthetic sea water from 273.15 to 298.15 K. Deep Sea Research Part A 37: 755-766.

Downing JA, McClain M, Twilley R, Melack JM, Elser J, Rabalais NN, Lewis WM, Turner RE, Corredor J, Soto D, Yanez-Arancibia A, Kopaska JA and Howarth RW (1999) The impact of accelerating land-use change on the N-cycle of tropical aquatic ecosystems: current conditions and projected changes. Biogeochemistry 46:109-148.

Elskens M, Penninckx MJ, Vandeloise R and Vanderdonckt E (1988) Use of a Simplex Technique and Contour Diagrams for the Determination of the Reaction-Rate Constants between Glutathione and Thiram in the Presence of Nadph. International Journal of Chemical Kinetics 20 (11):837-848.

Elskens M, Baeyens W, Brion N, De Galan S, Goeyens L and de Brauwere A (2005) Reliability of N flux rates estimated from $^{15}N$ enrichment and dilution experiments in aquatic systems. Global biogeochemical cycles 19: GB4028, doi:10.1029/2004 GB002332.

Elskens I and Elsken M (1989) Handleiding voor de bepaling van nutrienten in zeewater met een Autoanalyser IIrm system. Vrije Universiteit Brussel, pp 50.

Frankignoulle M and Borges AV (2001) European continental shelf as a significant sink for atmospheric carbon dioxide. Global Biogeochemical Cycles, 15:569-576.

Frankignoulle M, Borges AV and Biondo R (2001) A new design of equilibrator to monitor carbon dioxide in highly dynamic and turbid environments. Water Research 35:1344-1347.

Frankignoulle M, Abril G, Borges A, Bourge I, Canon C, Delille B, Libert E, and Théate JM (1998) Carbon dioxide emission from European estuaries. Science 282:434-436.

Froelich PN (1988) Kinetic control of dissolved phosphate in natural rivers and estuaries: A primer on the phosphate buffer mechanism. Limnology and Oceanography 33: 649-668.

Gattuso J-P, Frankignoulle M and Wollast R (1998) Carbon and carbonate metabolism in coastal aquatic ecosystems. Annual Reviews of Ecological Systems 29:405-434.

Gazeau F, Gattuso J-P, Middelburg JJ, Brion N, Schiettecatte L-S, Frankignoulle M and Borges AV (2005). Planktonic and whole system metabolism in a nutrient rich estuary (the Schledt estuary). Estuaries 28:868-883.

Gordon DCJ, Boudreau PR, Mann KH, Ong J-E, Silvert WL, Smith SV, Wattayakorn G, Wulff F and Yanagi T (1996) LOICZ biogeochemical modeling guidelines. LOICZ reports & Studies 5:1-96.

GRASS Development Team (2006) Geographic Resources Analysis Support System (GRASS) Software. ITC-irst, Trento, Italy.

Grasshoff K, Ehrhardt M and Kremling K (1983) Methods of Seawater Analysis. Verlag Chemie, Basel.

Gypens N, Lancelot C and Borges AV (2004) Carbon dynamics and $CO_2$ air-sea exchanges in the eutrophicated coastal waters of the Southern Bight of the North Sea: a modelling study. Biogeosciences 1:561-589.

Harrison JA, Caraco N and Seitzinger SP (2005) Global patterns and sources of dissolved organic matter export to the coastal zone: results from a spatially explicit, global model. Glob. Biogeochem. Cycles 19, GB4S04, doi:10.1029/2005GB002480.

Herbert RA (1999) Nitrogen cycling in coastal marine ecosystems. FEMS microbiology review 23:563-590.

Hoppe H-G (2003) Phosphatase activity in the sea. Hydrobiol. 493: 187-200.

Hoppe H-G (1983) Significance of exoenzymatic activities in the ecology of brackish water: measurements by means of methylumbelliferyl-substrates. Mar. Ecol. Prog. Ser. 11:299-308.

Hulth S, Aller RC, Canfield DE, Dalsgaard T, Engstrom P, Gilbert F, Sundback K and Thamdrup B (2005) Nitrogen removal in marine environments: recent findings and future research challenges. Mar Chem 94:125-145.

Jahnke J (1989). The light and temperature dependence of growth rate and elemental composition of Phaeocystis globosa Scherffel and P. pouchetii (Har.) Lagerh. in batch cultures. Netherlands Journal of Sea Research 23:15-21.

Jansson M, Olsson H and Pettersson K (1988) Phosphatases; origin, characteristics and function in lakes. Hydrobiol 170:157-175.

Joiris C, Billen G, Lancelot C, Daro MH, Mommaerts J-P, Bertels A, Bossicart M and Nijs J (1982) A budget of carbon cycling in the Belgian coastal zone: relative roles of zooplankton, bacterioplankton and benthos in the utilization of primary production. Netherlands Journal of Sea Research 16:260-275.

Karl DM and Bailiff MD (1989) The measurement and distribution of dissolved nucleic acids in aquatic environments. Limnol. Oceanogr. 34:543-558.

Koenker R (2006) Quantreg: Quantile Regression. R package version 3.90. http://www.r-project.org.

Koroleff F (1969) Direct determination of ammonia in natural waters as indophenol blue. Int. Council Expl. Sea 9:19-22.

Laane RWPM, Svendsen E, Radach G, Groeneveld G, Damm P, Pätsch J, Danielssen DS, Føyn L, Skogen M, Ostrowski M and Kramer KJM (1996) Variability in fluxes of nutrients (N, P, Si) into the North Sea from Atlantic Ocean and Skagerrak. German Journal of Hydrography 48:401-419.

Labry C, Delmas D and Herbland A (2005) Phytoplankton and bacterial alkaline phosphatase activities in relation to phosphate and DOP availability within the Gironde plume waters (Bay of Biscay). J. Exp. Mar. Biol. Ecol. 318:213-225.

Lancelot C and Mathot S (1987) Dynamics of a Phaeocystis-dominated spring bloom in Belgian coastal waters. 1. Phytoplankton activities and related parameters. Marine Ecology-Progress Series 37:239-248.

Lancelot C, Spitz Y, Gypens N, Ruddick K, Becquevort S, Rousseau V, Lacroix G and Billen G (2005) Modelling diatom and Phaeocystis blooms and nutrient cycles in the Southern Bight of the North Sea: the MIRO model. Marine Ecology-Progress Series 289:63-78.

Lancelot C, Gypens N, Billen G, Garnier J and Roubeix V (2007) Testing an integrated river-ocean mathematical tool for linking marine eutrophication to land use: The Phaeocystis-dominated Belgian coastal zone (Southern North Sea) over the past 50 years. Journal of Marine Systems 64 (1-4):216-228.

Lenhart H and Pohlmann T (1997) The ICES-boxes approach in relation to results of a North Sea circulation model. Tellus 49A:139-160.

Lewin-Koh NJ, Bivand R, Pebesma EJ, Gómez Rubio V, Jagger T (2005). Maptools: tools for reading and handling shapefiles. R package version 0.5-4.

Liss PS and Merlivat L (1986) Air-sea exchange rates: introduction and synthesis. In: The role of air-sea exchanges in geochemical cycling. Edt Buat-Ménard P, pp. 113-118, Reidel.

Lüger H, Wanninkhof R, WallaceDWR and Körtzinger A (2006) $CO_2$ fluxes in the subtropical and subarctic North Atlantic based on measurements from a volunteer observing ship. Journal of Geophysical Research-Oceans 111: C06024, doi:10.1029/ 2005 JC003101.

Nausch M, Nausch G and Wasmund N (2004) Phosphorus dynamics during the transition from nitrogen to phosphate limitation in the central Baltic Sea. Mar. Ecol. Prog. Ser. 266:15-25.

Nieuwenhuize J, Maas YEM, Middelburg JJ (1994) Rapid analysis of organic carbon and nitrogen in particulate materials. Marine Chemistry 45 (3):217-224.

Nightingale PD, Malin G, Law CS, Watson AJ, Liss PS, Liddicoat MI, Boutin J and Upstill-Goddard RC (2000) In situ evaluation of air-sea gas exchange parameterizations using novel conservative and volatile tracers. Global Biogeochemical Cycles 14:373-387.

OSPARCOM (2000) Quality status report 2000. OSPAR commission, London, http://www.ospar.com.

Pella E (1991) Elemental Organic Analysis, part 2- State of the art. In: Interscience Elemental Analysis pp 8-11.

Pinheiro J, Bates D, DebRoy S and Sarkar D (2006) NLME: Linear and nonlinear mixed effects models. R package version 3.1-71.

Platt T, Gallegos CL and Harrison WG (1980) Photoinhibition of photosynthesis in natural assemblages of marine phytoplankton. J. Mar. Res. 38:687-701.

Prandle D, Hydes DJ, Jarvis J and McManus J (1997) The seasonal cycles of temperature, salinity, nutrients and suspended sediment in the southern North Sea in 1988 and 1989. Estuarine Coastal and Shelf Science 45 (5):669-680.

R Development Core Team (2006) R: A language and environment for statistical computing. R Foundation for Statistical Computing, Vienna, Austria. http://www.R-project.org.

Reid PC, Lancelot C, Gieskes WWC, Hagmeier E and Weichart G (1990) Phytoplankton of the North Sea and its dynamics-a review. Netherlands Journal of Sea Research 26:295-331.

Rousseau V, Leynaert A, Daoud N and Lancelot C (2002). Diatom succession, silicification and silicic acid availability in Belgian coastal waters (Southern North Sea). Marine Ecology-Progress Series 236:61-73.

Roy RN, Roy LN, Vogel KM, Portermoore C, Pearson T, Good CE, Millero FJ and Campbell DM (1993) The dissociation-constants of carbonic-acid in seawater at salinities 5 to 45 and temperatures 0 degrees-C to 45 degrees-C. Marine Chemistry, 44:249-267.

Schiettecatte L-S, Gazeau F, Van der Zee C, Brion N and Borges AV (2006) Time series of the partial pressure of carbon dioxide (2001-2004) and preliminary inorganic carbon budget in the Scheldt plume (Belgian coast waters), Geochemistry, Geophysics, Geosystems 7: Q06009, doi:10.1029/2005GC001161.

Schiettecatte L.-S., H. Thomas, Y. Bozec & A.V. Borges (2007) High temporal coverage of carbon dioxide measurements in the Southern Bight of the North Sea, Marine Chemistry, 106(1-2), 161-173

Schoemann V, Becquevort S, Stefels J, Rousseau V and Lancelot C (2005) Phaeocystis blooms in the global ocean and their controlling mechanisms: a review. Journal of Sea Research 53:43-66.

Sebastian M and Niell FX (2004) Alkaline phosphatase activity in marine oligotropic environments: implications of single-substrate addition assays for potential activity estimations. Mar. Ecol. Prog. Ser. 277:285-290.

Sempéré R, Charrière B, Van Wambeke F and Cauwet G (2000) Carbon inputs of the Rhône River to the Mediterranean Sea: Biogeochemical implications. Global Biogeochemical Cycles 14:669-681.

Siefert RL (2004) The role of coastal zones in global biogeochemical cycles. Eos 85:470.

Soetaert K and Herman PMJ (1995) Carbon flows in the Westerschelde estuary (The Netherlands) evaluated by means of an ecosystem model (MOSES). Hydrobiologia 311:247-266.

Solorzano L and Sharp JH (1980) Determination of total dissolved phosphorus and particulate phosphorus in natural waters. Limnol. Oceanogr. 25:754-758.

Thingstad TF, Skjodal EF and Bohne RA (1993) Phosphorus cycling and algal-bacterial competition in Sandsfjord, western Norway. Mar. Ecol. Prog. Ser. 99:239-259.

Thomas H, Bozec Y, Elkalay K and de Baar HJW (2004) Enhanced open ocean storage of $CO_2$ from shelf sea pumping. Science 304:1005-1008.

Valderrama JC (1981) The simultaneous analysis of total nitrogen and total phosphorus in natural waters. Marine Chemistry 10:109-122.

Van Bennekom AJ and Wetsteijn FJ (1990) The winter distribution of nutrients in the Southern Bight of the North Sea (1961-1978) and in the estuaries of the Scheldt and the Rhine/Meuse. Netherlands Journal of Sea Research 25:75-87.

Van Boekel WHM and Veldhuis MJW (1990) Regulation of alkaline-phosphatase synthesis in Phaeocystis sp. Marine Ecology-Progress Series 61:281-289.

van Der Zee C and Chou L (2005) Seasonal cycling of phosphorus in the Southern Bight of the North Sea. Biogeosciences 2:27-42.

Veldhuis MJW and Admiraal W (1987) Influence of phosphate-depletion on the growth and colony formation of Phaeocystis pouchetii. Marine Biology 95:47-54.

Venables WN and Ripley BD (2002) Modern Applied Statistics with S. Fourth Edition. Springer, New York. ISBN 0-387-95457-0.

Wanninkhof RH and McGillis WR (1999) A cubic relationship between air-sea $CO_2$ exchange and wind speed. Geophysical Research Letters 26:1889-1892.

Wanninkhof R (1992) Relationship between wind speed and gas exchange over the ocean. Journal of Geophysical Research 97:7373-7382.

Weiss RF (1974) Carbon dioxide in water and seawater: the solubility of a non-ideal gas. Marine Chemistry 2:203-215.

Wollast R (1983) Interactions in Estuaries and Coastal waters. In: Bolin B and Cook RB (Eds) The major Biogeochemical Cycles and their Interactions, Wiley and Sons.

Wollast R (1976) Transport et accumulation de polluants dans l'estuaire de l'Escaut. In: Nihoul JCJ and Wollast R (Eds). Projet Mer, Rapport Final, Vol 10, 196-218, Services du premier Ministre Programmation de la politique scientifique, Belgium.

Wright RT and Hobbie JE (1966) Use of glucose and acetate by bacteria and algae in aquatic ecosystems. Ecology 47:447-464.

Yentsch CS and Menzel DW (1963) A method for the determination of phytoplankton chlorophyll and phaeophytin by fluorescence. Deep-Sea Res. 10:221-231.

**SPSD II** (2000-2005)

**BELGIAN SCIENCE POLICY**

HEAD OF THE DEPARTMENT 'RESEARCH PROGRAMMES': NICOLE HENRY (UNTIL SEPTEMBER 2007)

DIRECTOR GENERAL 'RESEARCH AND APPLICATIONS' : DOMINIQUE FONTEYN (FROM APRIL 2006)

CONTACT PERSONS: DAVID COX

**FOR MORE GENERAL INFORMATION:**
SECRETARIAT: VÉRONIQUE MICHIELS
WETENSCHAPSSTRAAT 8, RUE DE LA SCIENCE
B-1000 BRUSSELS
TEL : +32 (0)2 238 36 13
FAX : +32 (0)2 230 59 12
EMAIL : MICH@BELSPO.BE